

**Waste Package Development  
Civilian Radioactive Waste Management System  
Management & Operating Contractor**

MOL.19961029.0024

**MGDS**

**WBS: 1.2.2.3**

**QA: L**

**DESIGN ANALYSIS**

**Title: Probabilistic External Criticality Evaluation  
(SCPB: N/A)**

**Document Identifier: BB0000000-01717-2200-00037 REV 00**

**Originators: Peter Gottlieb  
John Massari**

**Checker: J. K. McCoy  
J.W.Davis**

**Lead Design Engineer: P. Gottlieb**

**Department Manager: Hugh A. Benton**

## Design Analysis Cover Sheet

Complete only applicable items.

①

QA: L

Page: 1

Of: 48

<b>2. DESIGN ANALYSIS TITLE</b> Probabilistic External Criticality Evaluation (SCPB: N/A)			
<b>3. DOCUMENT IDENTIFIER (Including Rev. No.)</b> BB0000000-01717-2200-00037 REV00			<b>4. TOTAL PAGES</b> 48
<b>5. TOTAL ATTACHMENTS</b> 4		<b>6. ATTACHMENT NUMBERS - NO. OF PAGES IN EACH</b> I-14, II-18, III-9, IV-1 (see Sect. 9 for Att. list)	
	Printed Name	Signature	Date
<b>7. Originator</b>	P. Gottlieb	<i>P. Gottlieb</i>	5/31/96
	J. R. Massari	<i>J. R. Massari</i>	5/31/96
<b>8. Checker</b>	J. K. McCoy	<i>J. K. McCoy</i>	5-31-96
	J. W. Davis	<i>J. W. Davis</i>	5/31/96
<b>9. Lead Design Engineer</b>	P. Gottlieb	<i>P. Gottlieb</i>	5/31/96
<b>10. QA Manager</b>	D. M. Jenkins	<i>D. M. Jenkins</i>	05-31-96
<b>11. Department Manager</b>	Hugh A. Benton	<i>Hugh A. Benton</i>	5/31/96

**12. REMARKS**

Initial Issue

Summary of originator and checker responsibilities:

<u>Section(s)</u>	<u>Responsible Individual(s)</u>	<u>Checker(s)</u>
1.0, 3.0, 4.0	P. Gottlieb	J.K. McCoy
2.0, 5.0, 6.0	J.R. Massari	J.K. McCoy
7.1	P. Gottlieb	J.K. McCoy
7.2	P. Gottlieb	J.K. McCoy
7.3	P. Gottlieb	J.K. McCoy
7.4	P. Gottlieb	J.K. McCoy
7.5	P. Gottlieb	J.K. McCoy
7.6	P. Gottlieb	J.K. McCoy
8.0	P. Gottlieb	J.K. McCoy
9.0	J.R. Massari	J.K. McCoy
Att. I	P. Gottlieb	J.K. McCoy
Att. II	P. Gottlieb	J.K. McCoy/J.W. Davis
Att. III	J. R. Massari	J.K. McCoy

**Design Analysis Revision Record***Complete only applicable items.*

①

Page: 2

Of: 48

**2. DESIGN ANALYSIS TITLE****Probabilistic External Criticality Evaluation****3. DOCUMENT IDENTIFIER (Including Rev. No.)****BB0000000-01717-2200-00037 REV00****4. Revision No.****5. Description of Revision**

00

Initial Issue

1.	Purpose .....	5
2.	Quality Assurance .....	5
3.	Method .....	6
4.	Design Inputs .....	6
4.1	Design Parameters .....	7
4.1.1	Reserved .....	7
4.1.2	Pressurized Water Reactor (PWR) SNF Assembly Parameters .....	7
4.1.3	Reserved .....	7
4.1.4	WP Environmental Parameters from TSPA-95 .....	7
4.1.5	Spent fuel dissolution rate, as a function of aqueous environment .....	7
4.1.6	Tuff matrix porosity data .....	9
4.1.7	Fissile material solubility .....	10
4.1.8	Fossil Log Statistics From Club Mines .....	10
4.1.9	Constants and Other Miscellaneous Information Used .....	10
4.2	Criteria .....	10
4.3	Assumptions .....	11
4.4	Codes and Standards .....	16
5.	References .....	17
6.	Use of Computer Software .....	21
7.	Design Analysis .....	22
7.1	Background, External Criticality, and Far-Field External Criticality ..	22
7.2	Dissolution of Spent Nuclear Fuel and Mobilization of Fissile Nuclides .....	22
7.3	Effective fissile enrichment .....	24
7.4	Uranium deposit types and their maximum uranium concentrations .....	25
7.4.1	Types of uranium deposits .....	26
7.4.2	Maximum uranium concentrations from non-organic reducing zones, hydrothermal and zeolite deposition process .....	27
7.4.3	Maximum uranium concentrations resulting from reduction zones of organic origin .....	28
7.4.4	Maximum uranium concentrations which could occur beneath Yucca Mountain .....	29
7.5	Minimum critical mass/radius at Yucca Mountain .....	31
7.6	Upper bound on the Probability of Assembling a Critical Mass ....	35

7.6.1	Methodology .....	35
7.6.2	Probability of reducing material, $\Pr\{\text{cluster} \log\}$ .....	35
7.6.3	Probability of encountering a log, $\Pr\{\log\}$ .....	38
7.6.4	Calculation of expected number of criticalities .....	40
7.6.5	Adjustment for critical masses greater than a single waste package .....	41
7.7	Increase in radionuclide inventory .....	43
7.8	Possibility of autocatalytic criticality .....	44
8.	Conclusions .....	47
9.	Attachments .....	48

## **1. Purpose -**

This analysis is prepared by the Mined Geologic Disposal System (MGDS) Waste Package Development (WPD) department to provide a probabilistic evaluation of the potential for criticality of fissile material which has been transported from a geologic repository containing breached waste packages of commercial spent nuclear fuel (SNF). This analysis is part of a continuing investigation of the probability of criticality resulting from the emplacement of spent nuclear fuel in a geologic repository.

The principal objectives of this evaluation are: (1) to identify the range of possible concentrations of uranium which could be precipitated in the rock downstream (groundwater flow) from the repository, (2) to calculate the minimum critical masses of such concentrations (assuming a fissile enrichment of the uranium corresponding to the characteristics of commercial spent nuclear fuel, and assuming a concentration of water moderator consistent with the known porosity of the rock), (3) to estimate conservative upper bounds for the probability of occurrence of such critical masses, and (4) to estimate the consequences of any credible criticality and calculate the resulting risk, which is product of the probability of occurrence multiplied by the consequences.

## **2. Quality Assurance -**

The Quality Assurance (QA) program applies to this analysis. The work reported in this document is part of the probabilistic evaluation of the waste package (WP) and engineered barrier segment (EBS). This activity can affect the proper functioning of the Mined Geologic Disposal System (MGDS) waste package; the waste package has been identified as an MGDS Q-List item important to safety and waste isolation (pp. 5, 16, Ref. 5.1). The waste package is on the Q-List by direct inclusion by the Department of Energy (DOE); a QAP-2-3 evaluation has yet to be conducted. The work performed for this analysis is covered by a WPD QAP-2-0 work control Activity Evaluation entitled *Perform Probabilistic Waste Package Design Analyses* (Ref. 5.2). This QAP-2-0 evaluation determined that such activities are subject to *Quality Assurance Requirements and Description* (QARD) (Ref. 5.3) requirements. Applicable procedural controls are listed in the evaluation.

All design inputs which are identified in this document are for preliminary design and shall be treated as unqualified data; these design inputs will require subsequent qualification (or superseding inputs) as the waste package design proceeds. This document will not directly support any construction, fabrication or procurement activity and therefore is not required to be procedurally controlled as TBV (to be verified). In addition, the inputs associated with this analysis are not required to be procedurally controlled as TBV. However, use of any data from this analysis for

input into documents supporting procurement, fabrication, or construction is required to be controlled as TBV in accordance with the appropriate procedures.

### **3. Method -**

The following methods are used for this analysis:

- The rate of dissolution of SNF is computed as a function of pH using the formula used for this purpose in Total System Performance Assessment - 1995 (TSPA-95, Ref 5.18).
- The mobilization rate of fissile nuclides is computed as the product of the maximum solubility limit multiplied by the flow rate of water through the waste package. This approximation *assumes that over the long term the solubility falls within the range specified by TSPA-95 (Ref. 5.18), and* repeated in Table 4.1-3 of this document.
- Flow in the saturated zone is computed using the TSPA95 plume dispersion methodology.
- A representative set of configurations which have some likelihood of being critical, is generated using a systematic methodology combining the probabilities estimated by the above methods. The criticality for each of these configurations is estimated from Monte Carlo neutronics calculations of the effective neutron multiplication factor,  $k_{eff}$ .
- The probability distribution of uranium deposit densities which could result from the encounters of groundwater containing dissolved fissile nuclides with the reducing zones (if any) is computed as the product of two probabilities: (1) the fraction of the area beneath the repository which could be occupied by reducing zones, the estimate of which is obtained by some comparison with natural uranium deposits (which are not actually analogs, but which can serve as a conservative probability basis) such as Pena Blanca and the Colorado plateau, (2) the probability of juxtaposition (or accumulation) of organic material modeled by individual logs which are randomly located throughout a typical mineralized zone (with the distribution parameters determined by the analysis of a map showing the location of the logs in one major deposit).

Further detail on the specific analytical methods employed for each step is available in Section 7 of this analysis.

### **4. Design Inputs -**

All design inputs are for preliminary design; these design inputs will require subsequent qualification (or superseding inputs) as the waste package design proceeds to final design.

**4.1 Design Parameters -****4.1.1 Reserved****4.1.2 Pressurized Water Reactor (PWR) SNF Assembly Parameters**Initial Uranium Loading per assembly (Ref. 5.7)

Maximum (Babcock & Wilcox Mark B):	464 kg
Average	434 kg

(Average is computed from total projected PWR Uranium mass divided by total projected number of PWR assemblies.)

Table 4.1-1. Amounts in grams/metric ton (g/MTU) of selected isotopes in 10 year old commercial SNF (Ref. 5.30)

Isotope	3% Initial Enrichment, 20 GWd/MTU Burnup	4% Initial Enrichment, 40 GWd/MTU Burnup
<sup>235</sup> U	1.302E4	9.689E3
<sup>238</sup> U	9.559E5	9.139E5
<sup>239</sup> Pu	4.534E3	6.342E3

**4.1.3 Reserved****4.1.4 WP Environmental Parameters from TSPA-95 (Ref. 5.18, p. 7-27)**

Max. Infiltration Rate for Low Inf. Scenario: 0.25 mm/yr

Max. Infiltration Rate for High Inf. Scenario: 10.0 mm/yr

(Maximum infiltration rate occurs at 50,000 years in TSPA-95 model)

**4.1.5 Spent fuel dissolution rate, as a function of aqueous environment**

The spent fuel dissolution rates used in this analysis are based on the model given in TSPA-95 (Ref. 5.18, p. 6-2),

$$\log R_{SF} = 7.323 - \frac{1585.2}{T} + 0.2621 \log(CO_3) - 0.1140 pH$$

where  $R_{SF}$  is the intrinsic dissolution rate of spent fuel (mg/m<sup>2</sup>day), T is the temperature (K), and  $CO_3$  is the total carbonate concentration (including



bicarbonate and carbonic acid) of the contacting groundwater (M).

The mean pH of J-13 well water has been found to be 7.6, and the mean carbonate concentration has been found to be 0.002M (Ref. 5.45). Table 4.1-2 lists the SNF dissolution rates calculated using the above model for the range of pH and carbonate concentration. The spent fuel pellet geometric specific surface area was taken to be the 39.6 cm<sup>2</sup>/g used in TSPA-95 (Ref. 5.18, p. 6-3)

Table 4.1-2. SNF Dissolution Rate (g/m<sup>2</sup>/yr) as a function of pH and CO<sub>3</sub> concentration at 30°C

pH\CO <sub>3</sub>	0.0002 M	0.002 M	0.02 M
6	1.01	1.84	3.37
6.5	0.88	1.62	2.96
7	0.78	1.42	2.59
7.5	0.68	1.24	2.27
8	0.60	1.09	1.99
8.5	0.52	0.96	1.75
9	0.46	0.84	1.53

#### 4.1.6 Tuff matrix porosity data (beta distributions)

Reference 5.25 provides distributions for the matrix porosity of various geologic members within Yucca Mountain. For the Calico Hills Non-Welded Zeolitic member, the porosity is described by a beta distribution with the parameters  $\alpha=32.317$ ,  $\beta=32.315$ , minimum = 0.05, and maximum = 0.562. Figure 4.1-1 below gives the cumulative distribution function described by the above beta distribution parameters.

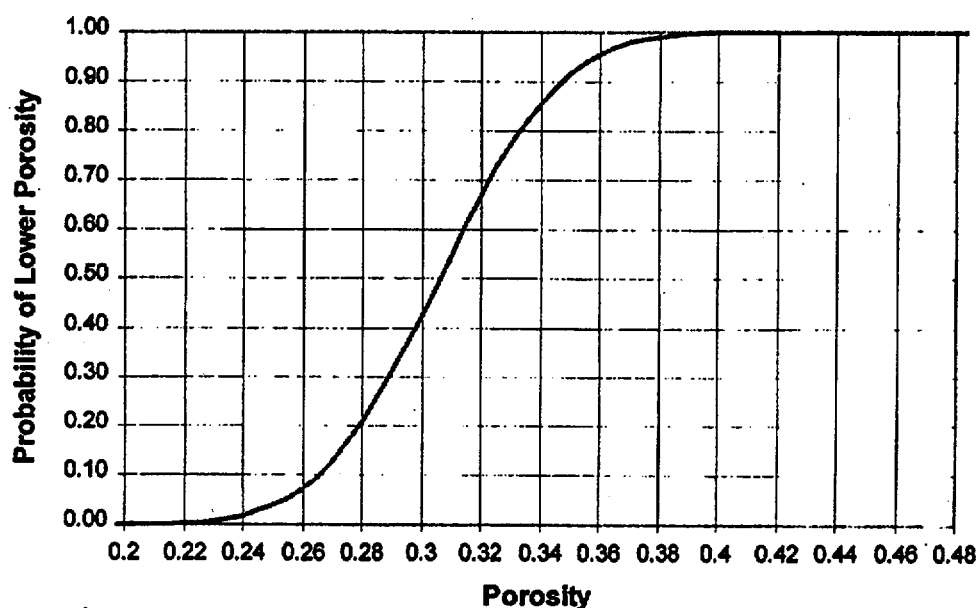


Figure 4.1-1. Matrix porosity distribution for Calico Hills non-welded zeolitic tuff (Ref. 5.25)

It should be noted that this table represents an adjustment from the raw data to eliminate a suspect outlier, which was 0.47 (Ref. 5.25, p. 7-10). Although not directly used in this document, the outlier was used as the basis for the worst case criticality analyses in Ref. 5.43.

**4.1.7 Fissile material solubility**

**Table 4.1-3. Fissile material solubilities (ppm) from TSPA-95  
(Ref. 5.18, p. 6-29)**

Element	Minimum	Mean	Maximum
Uranium	2.4E-3	7.6	2.4E3
Plutonium	2.4E-3	1.2E-1	2.4E-1

**4.1.8 Fossil Log Statistics From Club Mines**

This information is contained in Attachment III.

**4.1.9 Constants and Other Miscellaneous Information Used**

<sup>239</sup>Pu Half-life: 24,390 years (Ref. 5.20, p. 643)

**Advanced Uncanistered Fuel (AUCE) WP Dimensions**

Inner Diameter: 1409.7 mm (Attachment IV)  
Inner Lid-to-lid Length: 4585 mm (Attachment IV)

**4.2 Criteria -**

The repository criticality control design criteria for waste packages are based upon criteria from requirements documents. The criteria cited in requirement documents that have bearing on this analysis include:

**4.2.1 From the EBDRD (Reference 5.12);  
"3.2.2.6 CRITICALITY PROTECTION**

- A. The Engineered Barrier Segment shall be designed to ensure that a nuclear criticality accident is not possible unless at least two unlikely, independent, and concurrent or sequential changes have occurred in the conditions essential to nuclear criticality safety. Each system shall be designed for criticality safety under normal and accident conditions. The calculated effective multiplication factor must be sufficiently below unity to show at least a five percent margin, after allowance for the bias in the method of calculation and the uncertainty in the experiments used to validate the methods of calculation. [MGDS-RD 3.2.2.6.A][10CFR60.131(b)(7)]"

This study is performed for accumulations of material external to the Engineered

Barrier Segment (EBS). Therefore, the five percent margin required for evaluation of the EBS is not applied in calculating critical parameter in this study.

4.2.2 The Waste Package Implementation Plan (WPIP) (Reference 5.13) briefly echoes the criteria from the EBD RD. One of the design goals stated in the WPIP is to "Ensure subcriticality" (Reference 5.13, Page 2-5, Table 2-1).

#### 4.3 Assumptions -

4.3.1 For purposes of this analysis only, it is assumed that the waste package barriers and cladding have been sufficiently breached/degraded that the dissolution and removal from the waste package can proceed as if they were not there. The reason for this assumption is that it is expected that there will be a significant number of waste packages experiencing such degradation within 10,000 years following closure (Ref. 5.18), so it forms a reasonable basis for the computation of the upper bound for the probability of external criticality, since it is also a necessary assumption for the occurrence of any external criticality. This assumption is used in Section 7.2. There has, as yet, been no definitive estimation of the probability of occurrence of such degradation or of the expected number of such degradations in the repository. In fact, under some reasonable (but non-conservative) assumptions of barrier corrosion rates, many, if not most, of the waste packages will remain intact well beyond 100,000 years (Ref. 5.18).

4.3.2 It is assumed that, for the time periods of interest in this study, most of the  $^{239}\text{Pu}$  will decay to  $^{235}\text{U}$ . The basis for this assumption is the 24,390 year half-life of  $^{239}\text{Pu}$ . This assumption is used in Section 7.2 and is the basis for the criticality calculations of Ref. 5.43, which are used in Section 7.5.

4.3.3 For most of the calculations involving isotopic composition of SNF, it is assumed that the SNF is PWR criticality design basis fuel, 3% initial enrichment and 20 GWd/MTU burnup. The reason for this assumption is that this design basis fuel is more stressing with respect to criticality than all but the 2% of the expected SNF which has the highest fissile content. This is demonstrated by a combination of the analysis of design basis fuel in Ref. 5.10 and the presentation of fissile content in Ref. 5.43. The former reference gives a formula for  $k_{\infty}$  as a function of age, burnup, and initial enrichment and tabulates fuel percentile as a function  $k_{\infty}$  for the commercial SNF expected at the repository. The latter reference gives % fissile for several fuel types. The combined data is given in Table 7.6-3, which is some evidence that % fissile is directly proportional to  $k_{\infty}$  for these typical cases.

Although this table suggests a relationship between % fissile and  $k_{\infty}$ , no specific relationship between SNF percentile and % fissile has been established. Until a more thorough analysis leading to a specific relationship has been conducted, the relationship given in Table 7.6-3 will have to be interpreted as limited to the three fuel types listed, and more general interpretation will have to be considered TBV. This assumption is used in Sections 7.3 and 7.6.4 and in Attachment II.

- 4.3.4 A maximum solubility of Pu equal to 0.12 ppm was assumed, together with the assumption that colloids do not significantly enhance solubility/removal rate. The basis for the solubility assumption is Ref. 5.18, p. 6-29, and Table 4.1-3 of this document, which is derived from it, and the colloid assumption is consistent with assumptions in that reference and other treatments of the subject. This assumption is used only in Section 7.3, so any questions regarding it would not affect the rest of the document or its conclusions. Although the selected value is not the maximum of the possible range, and although the value could be increased by the occurrence of colloidal suspension of Pu, the assumption is considered conservative because a faster removal of Pu would increase its co-migration with the still faster migrating  $^{238}\text{U}$ . The latter would act as a neutron absorber to limit the likelihood of any external criticality.
- 4.3.5 It is assumed that the natural processes which precipitated uranium concentrations in the past will have the greatest probability of precipitating uranium in the future. This is based on the further assumption that the most probable uranium deposition processes and deposit types have been identified. This assumption is used in Section 7.4, 7.6, and Attachment II.
- 4.3.6 It is assumed that uranium bearing groundwater is enriched in hexavalent uranium (uranyl) from some upstream source of uranium. The basis for this assumption is that it is a common part of the mineralization process, and is discussed in the references cited in the section of the text using this assumption. This assumption is used in Section 7.4.1.
- 4.3.7 For calculation purposes it will be assumed that carbonaceous logs could exist at the base of the tuff in Yucca Mountain (which is approximately 1 km below the repository) and in the concentration which appears on the Colorado Plateau. It is also assumed that any distribution of logs which did occur at the base of the tuff would not have a higher concentration than those found on the Colorado Plateau. The single deep hole drilled to the base of the tuff at Yucca Mountain gives no indication of the necessary reducing material. However, the probability of encountering such an orebody, or reducing zone with potential for mineralization, can be estimated, according

to the methodology of Section 7.6.3, as the typical orebody area divided by the total sample space area ( $0.087 \text{ km}^2 / 1.24 \text{ km}^2 = 0.07$ ), so there is no strong evidence that such a reducing zone does not exist. On the other hand, if such reducing zone concentrations did exist they would not be likely to be greater than the concentrations which caused the deposits on the Colorado Plateau and in Wyoming, because extensive geologic and mining exploration throughout the United States have found no other large deposits with logs mineralized to such high concentrations. This assumption is used in Sections 7.4.4.1 and 7.6.3.

- 4.3.8 It is not considered possible to have any significant organic accumulation within the tuff. The basis of this assumption is that the hot ash would have oxidized any organic material as it was deposited. The organic accumulations in tuff elsewhere in Nevada are attributable to some layers of sedimentary rock between, or beneath, the layers of tuff. This assumption is used in Sections 7.4.4.1 and 7.6.3.
- 4.3.9 For calculation purposes only, it is assumed that the uranyl ion could replace all the Ca ion in the clinoptilolite. The basis of this assumption is that it is theoretically possible. However, experiments do not support such a wholesale replacement, as is indicated in Ref. 5.48. This assumption is used in Section 7.4.4.2.
- 4.3.10 The following specific parameter values are used only for the calculation of maximum possible replacement of Ca by U in clinoptilolite: (1) both tuff and clinoptilolite have a density of approximately  $2.52 \text{ g/cm}^3$ , (2) the solid rock is 70% clinoptilolite and 30% tuff or other mineral phases, and (3) the rock has 30 vol% porespace which is filled with water (typical of the saturated zone, and also a requirement for any criticality to occur). The basis for 70% clinoptilolite is that it is the upper limit of the range given in Ref. 5.47, p. 35. This is used as a volume percent, even though the reference intends it as a weight percent, because both the tuff and the clinoptilolite are assumed to have the same density. The basis for the water concentration is that it is close to the median given in 4.1.6, above. This assumption is used in Section 7.4.4.2.
- 4.3.11 It is assumed that none of the SNF neutron absorbers (primarily fission products) are transported in the uranium-bearing groundwater from the repository. This assumption is based on the further assumption that the neutron absorbers have either been removed from the SNF matrix much earlier than the fissile nuclides, or have remained in the matrix after removal of the fissile material. The basis for this assumption is that it is conservative. It is also technically justified by the fact that the neutron

absorbers generally have quite different solubilities from the uranium. This assumption is used in Section 7.5.

- 4.3.12 It is assumed that the organic deposits which can accumulate to form a reducing zone capable of capturing a critical mass from uranium bearing groundwater can be modeled by the juxtaposition of individual carbonaceous logs. It is further assumed that the mass provided by the uranium adsorption capability of a single log will be insufficient for criticality. The basis for the first part of this assumption is given in Section 7.6.2. The basis of the second part of the assumption is provided by neutronics calculation of the  $k_{eff}$  for a worst case cylinder, the details of which are described in Ref. 5.43, and summarized in Attachment II, and Section 7.6.2 of this document. This assumption is used in Section 7.6 and Attachment II.
- 4.3.13 For the most conservative estimate of possible organic log density beneath Yucca Mountain it is assumed that the sample space for the distribution is a typical buried river channel found on the Colorado Plateau and diagrammed in Ref. 5.31, and that such a buried river channel exists at the base of the tuff beneath Yucca Mountain. The basis of this assumption is that it is possible, and it is conservative. This assumption is used in Section 7.6.3, where it is also further explained.
- 4.3.14 For a less conservative estimate of possible organic log density beneath Yucca Mountain it is assumed that the sample space for the distribution of organic deposits (to be found at the base of the tuff under Yucca Mountain) is the entire geologic formation containing log deposits in orebodies on the Colorado Plateau. The quantification of this assumption rests on the simple counting of the orebodies in the geologic formation by Chenoweth (Ref. 5.41), which has not been formally documented or reviewed, and must, therefore be considered TBV. The basis of this assumption is that it conforms with geologic practice. The assumption is used for comparison purposes only in Table 7.6-2, and the more conservative alternative is used in all the subsequent calculations. This assumption is used in Section 7.6.3, where it is also further explained.
- 4.3.15 It is assumed for calculation purposes only that the waste packages are loaded homogeneously, so that high fissile fuel tends to be packaged together. The basis of this assumption is that it is somewhat likely, since fuel from the same batch will be likely to arrive at the repository together, or be loaded into a sealed multi-purpose canister (MPC) type container at the reactor together. It is also conservative, since spreading the fuel with high fissile content will dilute its effect and reduce the risk of criticality,

internal or external. This assumption is used in Section 7.6.4.

- 4.3.16 For purposes of estimating the maximum concentration of uranium in groundwater at the water table, it is assumed that the groundwater which has passed through a waste package flows vertically downward through the unsaturated zone with no dispersion of the concentration front, so that the uranium concentration in a groundwater stream from the repository is equal to the concentration at the waste package. Although there must always be some dispersion in natural systems, the basis of this assumption is that it is conservative. This assumption is used in section 7.6.5.
- 4.3.17 For purposes of estimating the maximum concentration of uranium in the water of the saturated zone, it is assumed that the concentration of uranium will spread according to the standard plume dispersion model. It is further assumed that the region of interest is the vertical projection of the plume centerline,  $y=0$ . The basis of this assumption is that it is possible and conservative. The basis of this assumption is given in Section 7.6.5, where it is used. Section 7.6.5 is for illustrative purposes only; the assumptions and results to not affect the rest of the document or its conclusions.
- 4.3.18 It is assumed that the increment of burnup provided by the external criticality is proportional to the reduction in fissile content of the fuel. The basis of this assumption is that it is consistent with the neutron depletion calculations done thus far. It should be considered to be TBV. This assumption is used in Section 7.7. This section is for illustrative purposes only; the assumptions and results to not affect the rest of the document or its conclusions.
- 4.3.19 It is assumed that the increase in radionuclide inventory for an external criticality is proportional to the increment of burnup. The basis for this assumption is that it is consistent with the waste package internal criticality evaluated in Ref. 5.50. It should be considered TBV. This assumption is used in Section 7.7. This section is for illustrative purposes only; the assumptions and results to not affect the rest of the document or its conclusions.
- 4.3.20 It is assumed that the logs are uniformly, and independently, distributed throughout the mineralized orebody in which they are found. The basis for this assumption is that it is verified by analysis of the Fischer map data (Ref. 5.28) in Attachments II & III. The assumption is used in Attachment II and Section 7.6.3.



4.3.21 It is assumed that a log will only be able to overlap the critical mass circle if its center is located so that the end of the log can overlap the critical mass circle center ( $r < l/2$ , where  $l$  is the length of the log). The basis of this assumption is that it is conservative (all logs reaching the center will be counted as going all the way through) and non-conservative (all logs overlapping the circle but not reaching the center will be discarded) aspects approximately cancel. This assumption is used in Attachment II.

4.3.22 In the algorithm for determining the number of intersecting logs required for criticality, it is assumed that only the fraction of the total log length defined by the segment of length  $(2/\pi)$  times the diameter of the adjusted critical mass circle will contribute to the critical mass. The basis of this assumption is given in the justification of the adjustment methodology, in Attachment II. This assumption is used in Attachment II.

#### 4.4 Codes and Standards -

Not applicable.

**5. References -**

- 5.1 *Q-List*, YMP/90-55Q, REV 3, Yucca Mountain Site Characterization Project
- 5.2 Activity Evaluation, *Perform Probabilistic Waste Package Design Analyses*, Document Identifier Number (DI#): BB0000000-01717-2200-00030 REV 02, CRWMS (Civilian Radioactive Waste Management System) M&O (Management and Operating Contractor)
- 5.3 *Quality Assurance Requirements and Description*, DOE/RW-0333P, REV 5, Department of Energy (DOE) Office of Civilian Radioactive Waste Management (OCRWM)
- 5.4 Kastenbergl, W.E., Peterson, P.F., Bessinger, B., Burch, J., Casher, G., Chambre, P., Cook, N.G.W., Doyle, F.M., Greenspan, E., Hilbert, B., Olander, D.R., Vujic, J., Mechanisms for Autocatalytic Criticality of Fissile Materials in Geologic Repositories, Summary Report - Rev. 0, Department of Nuclear Engineering, University of California, Berkeley, UCB-NE-4209, January 22, 1996.
- 5.5 *Reserved.*
- 5.6 *Reserved*
- 5.7 *Characteristics of Potential Repository Wastes*, DOE/RW-0184-R1, Volume 1, p. 2A-8, July 1992, DOE OCRWM
- 5.8 Breger, I.A., The role of Organic Matter in the Accumulation of Uranium, in Formation of Uranium Ore Deposits, IAEA-SM-183/19, International Atomic Energy Agency, 1974
- 5.9 Adler, H.H., Concepts of Uranium Ore Formation in Reducing Environments in Sandstones and Other Sediments, in Formation of Uranium Ore Deposits, IAEA-SM-183/43, International Atomic Energy Agency, 1974
- 5.10 *Waste Package Design Basis Fuel Analysis*, DI#: BBA000000-01717-0200-000121 REV 00, 1994, CRWMS M&O
- 5.11 *Reserved.*
- 5.12 *Engineered Barrier Design Requirements Document*, YMP/CM-0024, REV 0, ICN 1, Yucca Mountain Site Characterization Project

- 5.13 *Waste Package Implementation Plan, YMP/92-11Q, REV 1, Yucca Mountain Site Characterization Project*
- 5.14 Goodell, P.C., *Geology of the Pena Blance Uranium Deposits, Chihuahua, Mexico*, from *Uranium in Volcanic and Volcaniclastic Rocks, AAPG Studies in Geology No. 13, 1981*
- 5.15 Chenoweth, W.L. *The Uranium-Vanadium Deposits of the Uravan Mineral Belt and Adjacent Areas, Colorado and Utah*, New Mexico Geological Society Guidebook, 32nd Field Conference, Western Slope Colorado, 1981, pg 165-170.
- 5.16 French, D.E., *Origin of Oil in Railroad Valley, Nye County, Nevada*, The Wyoming Geological Association Earth Science Bulletin, 16, 1983 (pg 9-21)
- 5.17 *Reserved.*
- 5.18 *Total System Performance Assessment - 1995: An Evaluation of the Potential Yucca Mountain Repository*, DI#: B00000000-01717-2200-00136 REV 01, CRWMS M&O
- 5.19 George-Aniel, B., Leroy, J.L., Poty, B., *Volcanogenic Uranium Mineralizations in the Sierra Pena Blanca District, Chihuahua, Mexico: Three Genetic Models*, Economic Geology, 86, March-April 1991, pg 233-248.
- 5.20 Lamarsh, J.R., *Introduction to Nuclear Engineering*, 2nd Edition, Addison-Wesley Publishing Company, 1983
- 5.21 Finch, W.I., Butler, A.P.Jr., Armstrong, F.C., Weissenborn, A.E., Staatz, M.H., Olson, J.C., *Nuclear Fuels*, from *United States Mineral Resources*, Ed. Brobst, D.A., Pratt, W.P., United States Geologic Survey Prof. Paper 820, 1973
- 5.22 *Reserved.*
- 5.23 Castor, S.B., Berry, M.R., *Geology of the Lakeview Uranium District, Oregon*, from *Uranium in Volcanic and Volcanoclastic Rocks, AAPG Studies in Geology No. 13, 1982*, pp. 55-62.
- 5.24 Schrader, E. *Relationships between Uranium and trace metal concentrations in volcanic rocks from Nevada*, Economic Geology, 72, p104-107, 1977
- 5.25 *Total-System Performance Assessment for Yucca Mountain - SNL Second*

*Iteration (TSPA-93), Sandia National Laboratory, SAND93-2675, April 1994*

5.26 *Reserved.*

5.27 Garside, L.J., Radioactive mineral occurrences in Nevada, Nevada Bureau of Mines and Geology, Bulletin 81, 1973

5.28 Fischer, R.P., Vanadium Deposits of Colorado and Utah, Geological Survey Bulletin 936-P, 1942.

5.29 Hess, F.L., Uranium, Vanadium, Radium, Gold, Silver, and Molybdenum Sedimentary Deposits, in Ore Deposits of the Western States, Lindgren Volume of The American Institute of Mining and Metallurgical Engineers, New York 1933.

5.30 *Characteristics Database LWR Radiological PC Database, Version 1.1, CSCI A00000000-02268-1200-20002, CRWMS M&O*

5.31 Thamm, J.K., Kovschak, A.A., Adams, S.S., Geology and Recognition Criteria for Sandstone Uranium Deposits of the Salt Wash Type, Colorado Plateau Province, Prepared for the U.S. Department of Energy, Grand Junction Office, Colorado, GJBX-6(81), January 1981.

5.32 *Reserved.*

5.33 *Reserved.*

5.34 Smellie, J., The Fossil Nuclear Reactors of Oklo, Gabon, Radwaste Magazine, March 1995, pg 18-27.

5.35 Bowman, C.D., and Venneri, F., Underground Supercriticality from Plutonium and Other Fissile Material, Science & Global Security, 5, 1996 (pg 279-322)

5.36 *User Manual for the CDB\_R, DI#: A00000000-01717-2002-20002 REV 01, CRWMS M&O*

5.37 *Reserved.*

5.38 *Reserved.*

5.39 Gascoyne, M., Geochemistry of the Actinides and Their Daughters, in Uranium Series Disequilibrium: Applications to Environmental Problems, ed M.Ivanovich and R.S.Harmon, Clarendon Press - Oxford, 1982

- 5.40 Brinck, J.W., The Geologic Distribution of Uranium as a Primary Criterion for the Formation of Ore Deposits, in Formation of Uranium Ore Deposits, IAEA-SM-183/19, International Atomic Energy Agency, 1974.
- 5.41 Gottlieb, P., Estimate of mineralized areas, Interoffice Correspondence, LV.WP.PG.05/96-120, May 30, 1996.
- 5.42 NRC Staff Comments on the Report "Underground Supercriticality From Plutonium and Other Fissile Material" by Drs. C.D.Bowman and F.Venneri, Los Alamos National Laboratory, transmitted to Lake Barrett with letter dated August 7, 1995.
- 5.43 Davis, J.W., External Criticality Analysis, Interoffice Correspondence, LV.WP.JWD.05/96.122, May 30, 1996.
- 5.44 Grow, J.A., Barker, C.E., Harris, A.G., Oil and Gas Exploration Near Yucca Mountain, Southern Nevada, High Level Radioactive Waste Management, Fifth Annual International Conference, ASCE & ANS, 1994, pg 1298-1315.
- 5.45 Pitting, Galvanic, and Long-Term Corrosion Studies on Candidate Container Alloys for the Tuff Repository, U.S. Nuclear Regulatory Commission, NUREG/CR-5709, January 1992.
- 5.46 Basinski, P. The Mineralogy and Uranium Potential of Bedded Zeolites in the Northern Reese River Valley, Lander County, Nevada, Master's degree thesis, University of Nevada Reno, December 1978.
- 5.47 Bish, D.L., Carey, J.W., Levy, S.S., Chipera, S.J., Mineralogy-Petrology Contribution to the Near-Field Environment Report MILESTONE LA3668, LA-EES-1-TIP-96-003, R1, March 1996.
- 5.48 Katayama, N., Kubo, K., Hirono, S., Genesis of Uranium Deposits of the Tono Mine, Japan, in Formation of Uranium Ore Deposits, IAEA-SM-183/19, International Atomic Energy Agency, 1974, pp. 437-452.
- 5.49 Davis, J., Fleming, M., King, J., FY95 CDA Update OFF Waste Stream Data, CRWMS M&O Contractor, Interoffice Correspondence SA.VA.JK.04/95.045, April 3, 1995.
- 5.50 Second Waste Package Probabilistic Criticality Analysis: Generation and Evaluation of Internal Criticality Configurations, DI#: BBA000000-01717-2200-00005 REV 00.

**6. Use of Computer Software -****A. Scientific and Engineering Software:**

The Characteristics Database (CDB) LWR Radiological PC Database, CSCI: A00000000-02268-1200-20002, Ver. 1.1 was used to obtain the isotopic characteristics of the criticality design basis SNF. The CDB has been qualified by the Office of Civilian Radioactive Waste Management for use in work subject to the requirements of the QARD (Ref. 5.3). The CDB was installed on an IBM-compatible PC in accordance with the User Manual for the CDB\_R (p. 1, Ref. 5.36) and was obtained in accordance with the QAP-SI series procedures. Use of the SNF isotopic characteristics from the CDB is appropriate for this design analysis and is within the range of validation performed for the CDB. The data extracted from the CDB are given in Section 4.1.2 and are used in Section 7.3.

**B. Computational Support Software:**

- 6.1 Microsoft Excel v5.0, loaded on a 66MHz 486 PC.
- 6.2 Microsoft Visual C++ compiler, version 1.0, loaded on a 66MHz 486 PC used as computational support software with Excel or MathCad checking to verify the algorithms used.

## **7. Design Analysis -**

This design analysis is presented in eight sections. Section 7.1 provides the background for this analysis. Section 7.2 describes the dissolution of SNF and the mobilization of fissile nuclides. Section 7.3 presents the results of analysis indicating the range of effective fissile enrichments as a function of time. Section 7.4 describes the maximum uranium concentrations existing in typical geologic environments and the maximum which could possibly occur beneath Yucca Mountain. Section 7.5 summarizes the calculations of minimum critical mass/radius for possible uranium concentrations which could result from operation of a repository at Yucca Mountain. Section 7.6 uses the previous results to derive upper bounds on the probability of natural processes assembling a critical mass beneath a repository at Yucca Mountain. Section 7.7 provides an estimate of the increased radionuclide inventory which could result from an external criticality. Section 7.8 provides an estimate of the possibility of autocatalytic criticality.

### **7.1 Background, External Criticality, and Far-Field External Criticality**

The near-field environment is defined as the engineered barrier segment (EBS) external to the waste package; the far-field environment is any portion of the rock of Yucca Mountain beyond the near field. This study focuses on far-field external criticality because an upper bound on the probability of accumulating a critical mass/configuration in the far-field can be calculated from analysis of existing uranium deposits. Evaluation of criticality in the invert will require geochemical calculations, and will be accomplished in future studies.

### **7.2 Dissolution of Spent Nuclear Fuel and Mobilization of Fissile Nuclides**

There are a number of isotopes in SNF which are neutronically active, either fissile or neutron absorbing. The long term criticality is fairly well characterized by the three isotopes  $^{238}\text{U}$ ,  $^{235}\text{U}$ , and  $^{239}\text{Pu}$ . The  $^{235}\text{U}$  is the principal fissile isotope and is much longer lived than any other fissile isotope; the  $^{239}\text{Pu}$  is the next most numerous fissile, and its fissile capability persists after its decay into  $^{235}\text{U}$ ;  $^{238}\text{U}$  is the most numerous neutron absorber in the SNF, and its chemical behavior is identical with  $^{235}\text{U}$  so it will co-migrate. The dissolution rate of the SNF pellets is mass controlled, so the determining parameter is the total material (Ref. 5.18). The rate of removal from the waste package will be seen to be solubility, or flux, controlled, and so will vary with species solubility. Therefore, removal from the waste package will be discussed in terms of these three principal isotopes.

The range of possible dissolution rates for the  $\text{UO}_2$  pellet material of commercial SNF is .46 to 3.37 g/m<sup>2</sup>/yr (Ref 5.18). Under the worst case assumption that the waste package barriers have been breached, all the cladding has failed, and that

water can contact the entire surface area of the  $\text{UO}_2$  pellets, the maximum surface area which can be exposed to the water is the product of the total mass of uranium per waste package (which is approximated by the initial heavy metal, which, in turn, is a maximum of 9,744,000 g total for the largest assembly type, 0.464 metric tons uranium (MTU), for a 21 PWR waste package) multiplied by the specific surface area per unit mass of a fuel pellet,  $39.6 \text{ cm}^2/\text{g}$  (Ref. 5.18, p. 6-3). Hence the range of possible dissolution rates for the entire waste package is 17.7 to 130.1 kg/yr. However, it will be seen below that the removal rate of uranium from the waste package is mainly solubility limited (also called flux limited) to rates much lower than this.

Mobilization, or removal, of fissile material is limited by both its solubility and by the flow rate through the waste package. In the SNF, uranium exists in the +4 valence or oxidation state (called the uranous ion). This oxidation state is very insoluble (only 1 ppb in very acidic conditions,  $\text{pH}=2$ , Ref 5.39, pp. 40-41). The SNF is degraded by oxidation to the +6 state ( $\text{UO}_2^{++}$ , called the uranyl ion), which has a solubility at least three orders of magnitude larger. The maximum rate of removal of uranium from the waste package is the product of the maximum solubility (2400 ppm, or  $2.4 \text{ kg/m}^3$ , Ref 5.18, p. 6-29) multiplied by the maximum infiltration rate (0.01 meters/yr, Ref 5.18, p. 7-27) and by the cross-section area which the waste package interior presents to the vertical infiltration ( $6.46 \text{ m}^2$ ), to give 0.155 kg/yr. Since this rate is much smaller than the range of dissolution rates (17.7 to 130.1 kg/yr) computed in the previous paragraph, the maximum uranium removal rate is said to be flux limited; this calculation shows the maximum removal rate is equal to 0.155 kg/yr of uranium per waste package.

The plutonium removal rate will be much slower, since its solubility limit is much smaller. However, it will be seen that the typical time for the removal from the waste package of the fissile material (which removal is necessary for any external criticality) will generally be longer than the  $^{239}\text{Pu}$  half-life, so, *for the time periods of interest in this study, most of the  $^{239}\text{Pu}$  will decay to  $^{235}\text{U}$*  and be removed according to the uranium chemistry. Under this assumption/approximation that most of the  $^{239}\text{Pu}$  will be removed as  $^{235}\text{U}$ , the removal time is determined by dividing the total mass of the three isotopes in a waste package ( $^{238}\text{U} + ^{235}\text{U} + ^{239}\text{Pu} = 9485.3 \text{ kg}$ ) by the uranium maximum removal rate of 0.155 kg/yr. This process gives approximately 61,200 years to remove all the uranium from the waste package. It should be noted that even though this is the most conservative (smallest) estimate of removal time, it is still more than twice the  $^{239}\text{Pu}$  half-life of 24,390 yrs so the approximation that all  $^{239}\text{Pu}$  decays to U before being removed from the waste package is justified. Nevertheless, this approximation does have a slight non-conservative aspect since  $^{239}\text{Pu}$  is slightly more neutron-efficient than  $^{235}\text{U}$  (specifically, it has a slightly higher fission cross-section for neutrons, and it releases slightly more neutrons per fission).



Using the more likely values for infiltration rate (1 mm/yr; mid-way between high and low infiltration scenario rates in Section 4.1.4) and solubility of uranium (7.6 ppm) the removal time for all the uranium from the waste package would be approximately 200 million years. Such a long time estimate may not be meaningful, since major geologic changes would be likely to effect the repository directly over such a long time. It should be noted, however, that many geologic formations have survived intact for over a billion years (one being the Oklo uranium deposit, to be discussed in Section 7.4 below).

### **7.3 Effective fissile enrichment**

The fact that Pu is much less soluble than U raises the question of whether the criticality potential of commercial SNF could be enhanced by selective removal of uranium, which is mostly the neutron absorbing form  $^{238}\text{U}$ . In fact, the Nuclear Regulatory Commission (NRC) has requested that such an analysis be included as part of the criticality licensing studies (Ref. 5.42, Consideration I.2, pp. 3,4). To answer this question, the coupled rate equations for  $^{238}\text{U}$ ,  $^{235}\text{U}$ , and  $^{239}\text{Pu}$  were integrated numerically using a "C" program. This analysis was performed using a range of values for the solubilities of uranium and plutonium and for the flow rate through the waste package. The equations also modeled the decay of  $^{239}\text{Pu}$  to  $^{235}\text{U}$ . The specific rate equations are given in Attachment I, as part of the "C" program listings and associated annotations.

The following parameters were used for all cases:

- Maximum concentration of Pu in solution, 0.12 ppm, which is the mean value given in Table 4.1-3.
- Infiltration rate, 10 mm/yr, which is the maximum listed in Section 4.1.4

The range of maximum U concentrations (maxu) was 100 ppm to 2400 ppm. The upper limit corresponds to the maximum in Table 4.1-3, and the lower limit has been chosen to cover the range of behaviors as will be seen below.

Isotopic compositions were determined for 2 fuel types for a PWR waste package with 21 assemblies having the largest assembly mass, 0.464 MTU/assy, and using the isotopic fractions given in table 4.1-1:

- The PWR criticality design basis fuel: 3% initial enrichment and 20 GWd/MTU burnup which gives, 9314.3 kg of  $^{238}\text{U}$ , 126.9 kg of  $^{235}\text{U}$  and 44.2 kg of  $^{239}\text{Pu}$  per waste package.
- 4% initial enrichment and 40 GWd/MTU burnup, which gives 8905.0 kg of  $^{238}\text{U}$ , 94.4 kg of  $^{235}\text{U}$  and 61.8 kg  $^{239}\text{Pu}$  per waste package.

The results are somewhat sensitive to the bookkeeping for  $^{239}\text{Pu}$ . Two cases are examined: (1)  $^{239}\text{Pu}$  having the same weight in fissile contribution as  $^{235}\text{U}$ , and (2)

$^{239}\text{Pu}$  having a factor of 1.25 (the approximate ratio of fissile cross-sections) times the contribution of  $^{235}\text{U}$ . Either condition could be operative, or some value in between, depending on the concentrations of uranium and moderator. In the following discussion these are called approximation A and B, respectively.

The for approximation A the calculations show the following three types of behavior for the effective enrichment (fissile content divided by total of all three isotopes).

1. For relatively low values of maxu (less than 150 ppm), the effective enrichment simply decreases slightly as a function of time. This is an artifact of the conversion from the mass of plutonium ( $^{239}\text{Pu}$ ) to the mass of uranium ( $^{235}\text{U}$ ) for the plutonium decay. Since the rate of removal of uranium is slower than the rate of decay of plutonium, most of the fissile is still remaining when all the  $^{239}\text{Pu}$  is gone (mostly from decay).
2. For intermediate values of maxu (typically 200 ppm) there is a slight increase of effective enrichment with time, reaching a maximum of less than 1% increase over the initial value, and then falling off slightly.
3. For high values of maxu (greater than 200 ppm) the effective enrichment increases with time, but by the time it has doubled, there are only a few kg of fissile left. Furthermore, when the fissile content has dropped to half its initial value (identified as Half in the outputs given in Attachment I), the increase in fissile content is less than 10%.

For approximation B, there are only two behavior regimes:

1. For relatively low values of maxu (less than 1200 ppm) the effective enrichment simply declines with time. This is primarily because the extra contribution of  $^{239}\text{Pu}$  (factor of 1.25) disappears as the  $^{239}\text{Pu}$  decays. Since the cases chosen for illustration have higher maxu than for approximation A, above, most of the fissile has been removed by the time Pu goes to zero.
2. For higher values of maxu (greater than 1200 ppm) the effective enrichment increases with time but, as with approximation A, above) the percent increase is only 10% (for the worst case of maxu = 2400 ppm) by the time the total fissile content has decreased by 50% (identified as Half in the outputs given in Attachment I).

These results show that it is not possible to remove the uranium fast enough for this effect to be significant.

#### **7.4 Uranium deposit types and their maximum uranium concentrations**

This section describes relevant uranium occurrences in tuff that is analogous to the rock at Yucca Mountain and in sedimentary rocks, which provide much higher grade ores. Subsection 7.4.4 describes how this information is used to build a model for

the upper bound of the probability of the existence of reducing zones which could exist beneath Yucca Mountain. This is based on the *assumption that the natural environments that accumulated uranium in the past will have the greatest probability of accumulating uranium in the future.*

#### **7.4.1 Types of uranium deposits**

The United States has approximately 30% of the world uranium reserves (J.W.Brinck, Ref 5.40, pg 22), and most is near the Four Corners area of the Colorado Plateau and in Wyoming. Brinck has also estimated the United States total of 259,000 metric tons consists of individual deposits averaging 2300 metric tons at an average ore grade is 0.195% (Ref 5.40, pg 23). A higher average ore grade has only been reported for one country, South Africa, 0.29% (Ref 5.21, p. 463 ), but that the size of those deposits is only 10% of the US.

The largest and richest uranium deposits worldwide are associated with organic material in sedimentary rock. This organic material provides a reducing substrate to convert the soluble hexavalent uranium to the insoluble quadrivalent form, particularly the mineral uraninite (pure  $\text{UO}_2$ ). The groundwater solution which flowed through the rock *is generally assumed to have been enriched in hexavalent uranium (uranyl) from some upstream source rock of higher uranium concentration.* The deposition substrate is either the organic material itself or  $\text{H}_2\text{S}$  (or some form of organic sulfur) generated by bacterial decay of the organic material. These deposits are found only in sedimentary rock, generally sandstone, but sometimes limestone. In one deposit (Oklo) the maximum ore grade of a small portion of the total deposit has been found as high as 60%; otherwise the local peak ore concentration has never been above 20% (Ref. 5.34, p. 20). Of course, individual uraninite nuggets would have uranium concentrations as high as 88%, but these are so small in dimension as to not even be recorded in the general literature.

Another major mechanism for uranium concentration is by deposition on fracture surfaces from hydrothermal (hypogenic) fluids which could have derived their uranium content directly from volcanic magma or from leaching of some nearby source rock. The precipitation from the hydrothermal fluid could be induced by cooling, by encountering an organic reducing zone, or by increased concentrations of inorganic ions (Ca or silicate) which can displace the uranyl from solution. This is the principal type of uranium concentration observed in tuff. Secondary enrichment can occur as uranium is mobilized in the weathering environment.

A third mechanism for uranium concentration is adsorption in zeolites. These are cage-like minerals which have structural channels that can exchange ions with aqueous solutions. Although this is a relatively rare type of uranium deposit, it is relevant to Yucca Mountain, because such a concentration has been observed in

clinoptilolite (a common zeolite) that is a major constituent of a tuff similar to that found at Yucca Mountain (Ref. 5.46), and because similar zeolites in tuff (not containing uranium) are fairly common at Yucca Mountain, with many of the drill holes showing zeolite deposits several meters thick and constituting 50 to 70% of the local rock (Ref. 5.47).

These general mechanisms are limited by available surface area for chemical-physical reaction between solution and host rock. For the organic-reduction mechanism the large surface area is provided by either microfractures in the bulk organic material itself (e.g. a log) or the fine interstices of sedimentary rock containing a more refined organic material with little internal surface area. For the hydrothermal mechanism the surface area is provided by extensive fracturing, which may be provided by the same hydrothermal process as provides the fluid or may have been pre-existing. For the zeolite exchange process, the effective surface area is provided by the cage structure of the zeolite itself.

#### **7.4.2 Maximum uranium concentrations from non-organic reducing zones, hydrothermal and zeolite deposition process**

The Pena Blanca uranium district, located 50 km north of Chihuahua City contains some of the richest uranium ore reported for tuff. The peak concentration of 9% uranium was found in a 13 cm diameter, very highly fractured breccia for a total uranium content of less than 3 kg  $\text{UO}_2$ . This particularly rich breccia sample is one of several characterized by P.C. Goodell (Ref 5.14, Table 3, with the size information from a private communication with the author), as part of the Nopal 1 deposit, which is a pipe like body 100 meters high with a 20 meter by 40 meter cross-section, and an average uranium concentration of .11%, as reported by George-Aniel et.al. (Ref 5.19, p. 238). The lower grades dominate the rest of the deposit; in fact, the latter reference does not even mention the 3 kg, 9% sample. The source rock for the lower grade deposits is believed to be rhyolites, which range from 10 to 35 ppm  $\text{U}_3\text{O}_8$ .

In the Pena Blanca district, only the peak 9% sample is believed to contain quadrivalent uranium (specifically uraninite,  $\text{UO}_2$ , Ref. 5.14, p. 286, uraninite being identified with this peak sample as "in the breccia"). Although even this high a grade is insufficient for criticality of commercial SNF, it is evidence of some strong organic type reduction from the hexavalent solution which would be necessary to precipitate the higher concentrations required for criticality. The remainder of the district in general, and the Nopal 1 deposit in particular, is the result of a deposition process which does not reduce the hexavalent ions, but only incorporates this hexavalent uranium into carbonate, silicate, and oxide minerals, particularly uranophane  $[\text{Ca}(\text{UO}_2)_2(\text{SiO}_3)_2(\text{OH})_2]$  (Ref. 5.14, p. 286). Similar low grade uranium deposits in tuff are found in Oregon (Ref 5.23, p. 55) and in Nevada (Ref 5.24, p.

104).

It is, therefore, concluded that there is very little likelihood of finding high organic concentrations in tuff, and those rare exceptions are likely to be small, like the 3 kg sample from Pena Blanca. However, there is a possibility of log-type organic deposits in basal pyroclastic deposits, as is discussed in Section 7.4.4.1, below.

A review of the best known uranium deposit in zeolite, the Tono mine in Japan, has been given by Katayama et.al. (Ref. 5.48). The maximum uranium concentration reported in this reference is .9%. This observed concentration is consistent with the maximum uranium concentration achieved in a laboratory experiment also reported by Ref. 5.48, p.448. In this experiment the uranium concentration in the zeolite was found to increase linearly with uranium concentration in the contacting water, corresponding to a partition coefficient of 700, and to saturate at just under 1% uranium in the zeolite for uranium concentration in the water above 100 ppm. The applicability of this mechanism to Yucca Mountain is discussed in Section 7.4.4.2, below.

#### **7.4.3 Maximum uranium concentrations resulting from reduction zones of organic origin**

The highest recorded grade of uranium ore, 60% was recorded at Oklo, Gabon. The original deposition of the uranium (over 2 billion years ago) is believed to have been due to the reduction of highly concentrated organic material, but the original organic material is no longer distinguishable as such, Smellie (Ref. 5.34, p. 19). On the other hand, the United States deposits with the highest concentrations of uranium ore generally contain organic material (or its fossilized remains) which is still identifiable.

Tabular deposits are of two types, peneconcordant (or true bulk) and roll-front (Ref. 5.9, p. 145). The former occupies a larger volume, but the latter is of higher concentration. This difference reflects the nature of the organic deposit responsible, either directly or indirectly, for the reducing zone which caused the uranium precipitation, the roll-front having been more concentrated than the peneconcordant. Neither of these types of tabular deposits has concentrations as high as the log type deposits, in which the boundaries of the organic material are still recognizable.

The summary of uranium deposits resulting from concentrated organic reducing zones has been given by Breger (Ref. 5.8); he reports a 64 element sample of mineral concentrations in logs primarily from the Colorado Plateau and Wyoming, with an average of 1.88% uranium (Ref 5.8, pp. 102-105). The maximum concentration among these samples is 16.5%. Other reports of maximum

concentration near 20% have been given by Hess (Ref. 5.29, p. 467) and Chenoweth (Ref 5.15, p. 168).

The mechanism responsible for the strong deposition capability of organic matter is demonstrated by measurements of the partition coefficient between organic matter (humic material in the form of peat and lignite) and U bearing groundwater, with values as high as  $10^4$ , as reported in studies cited in Ref 5.39, p. 44; subsequent experiments, identified in the same reference, also indicate that it is the organic surfaces and not the humic acid in porespace which cause the adsorption.

Detailed chemical and X-ray diffraction examination of uranium log samples shows both crystalline and non-crystalline material (the latter of which may be either colloidal material or amorphous solids (Breger Ref 5.8, p. 106). It should be noted that the crystallized mineralization usually only extends over a small fraction of the volume of the log. Furthermore, the uranium concentrations can vary by 2 orders of magnitude from one side of a log to the other, particularly if the logs were oriented perpendicular to the direction of groundwater flow during mineralization.

#### **7.4.4 Maximum uranium concentrations which could occur beneath Yucca Mountain**

##### **7.4.4.1 Applicability of other districts**

In a study of radioactive mineral occurrences in Nevada, L.J.Garside has suggested (Ref 5.27, p. 8) that, "charcoal carbonization of wood at the base of ash-flow tuffs [serves] as a precipitant for uranium." He also suggests that organic matter can serve as a food for anaerobic bacteria producing  $H_2S$  which is also an effective uranium reductant. However, there is no direct evidence of any uranium deposits in tuff resulting from this mechanism, and the same reference notes that the uranium deposits at Coaldale Prospect [a low-grade Tertiary occurrence in Miocene sedimentary rock some 200 km northwest of Yucca Mountain] are not replacement deposits.

Although oil occurs in Nevada, it is not likely to be a reductant for dissolved uranium at Yucca Mountain. Oil accumulations in Railroad Valley appear to have migrated from the Chainman Shale (Ref 5.16, p. 10), and are not likely to be duplicated at Yucca Mountain because the recent higher temperature history in that vicinity would have decomposed any oil (Grow et.al., Ref. 5.44, p. 1298). Therefore, the identified Nevada oil accumulations are not analogous to any known conditions at Yucca Mountain.

With this evidence, it could be assumed that the organic deposits in Nevada are too weak to reduce uranium to concentrations found on the Colorado Plateau, let alone

to the much higher concentrations found at Oklo. Nevertheless, since carbonaceous deposits of the log type do exist in Nevada at the base of ash-flow tuffs (Ref 5.27, p. 8), and since a recognized geologic study has suggested that they could serve as a precipitant, it will be prudent to include the possibility in this analysis. *For calculation purposes it will be assumed that logs could exist at the base of the tuff in Yucca Mountain (which is approximately 1 km below the repository) and in the concentration which appears on the Colorado Plateau. It is also assumed that any distribution of logs which did occur at the base of the tuff would not have a higher concentration than those found on the Colorado Plateau. It is not considered possible to have any significant organic accumulation within the tuff because the hot ash would have oxidized any organic material as it was deposited. The organic accumulations in tuff elsewhere in Nevada are attributable to carbonaceous material that occurs beneath the layers of tuff.*

Although a reducing zone in the form of organic logs is conservatively assumed to be possible at the unconformity beneath the tuffs at Yucca Mountain, any significant roll-front deposition in tuff must be considered to be very unlikely, because fractures rather than interstitial porosity are thought to control fluid flow. In contrast, the interconnected porous grain structure sandstone provides a more uniform permeability throughout the bulk of the rock.

#### **7.4.4.2 Potential for uranium concentration within the tuff at Yucca Mountain**

The maximum concentration of uranium which the zeolite clinoptilolite could accumulate by the ion-exchange mechanism from uranium-bearing groundwater at Yucca Mountain is most likely constrained by the maximum reported for natural deposits which have formed by this process. These maximum concentration occurrences include 0.5% at the Tono Mine in Japan (Ref. 5.48, pp. 445,446, Figure 9 and Table I), or 0.7% at the more closely analogous Northern Reese River Valley (Ref. 5.46), or just under 1%, the maximum observed in the laboratory using uranium saturated water (Ref. 5.48, p. 448).

For a maximum theoretically possible value, it is possible to make a more conservative estimate under the *assumption that the uranyl ion could replace all the Ca ion in the clinoptilolite*. Using the chemical formula for clinoptilolite,  $K_{0.6}Na_{0.2}Ca_3Al_{6.8}Si_{29.2}O_{72} \cdot 1.6H_2O$ , and replacing 3 Ca with 3  $UO_2$ , gives a uranium weight fraction of clinoptilolite of  $g_u = 0.236$ . The following assumptions are used to convert this weight fraction of clinoptilolite to a weight fraction of rock: (1) *both tuff and clinoptilolite have a density of approximately 2.52 g/cm<sup>3</sup>*, (2) *the rock matrix is 70 vol% clinoptilolite and 30 vol% other mineral phases*, and (3) *the rock has 30 vol% porespace which is filled with water*. These assumptions give the following volume fractions of the rock:

ordinary clinoptilolite	$v_{co} = .7*(1-.3) = 0.49$
tuff	$v_t = .3*(1-.3) = 0.21$
water	$v_w = 0.3$

If R is the ratio of the molecular weight of clinoptilolite with calcium replaced by uranium divided by the molecular weight of ordinary clinoptilolite ( $R = 1.245$ ), the overall density of the rock, with Ca replaced by  $UO_2$  and including water, is

$$\rho_R = 2.52(Rv_{co} + v_t) + v_w = 2.37$$

The weight and volume fractions of  $UO_2$  can then be computed from

$$w_{uo2} = g_u R \rho_{co} v_{co} / \rho_R = .149$$

$$v_{uo2} = w_{uo2} \rho_R / \rho_{uo2} = .032,$$

where  $\rho_{uo2}$  is the density of  $UO_2 = 10.96 \text{ g/cm}^3$  and  $\rho_{co}$  is the density of clinoptilolite =  $2.52 \text{ g/cm}^3$

Figure 7.5-1 shows that this volume fraction of  $UO_2$  gives a  $k_{\infty}$  less than 0.88, so it is impossible to form a critical mass from zeolite in tuff, even if all the Ca is replaced by commercial SNF  $UO_2$  from uranium bearing groundwater.

#### **7.4.4.3 Potential uranium concentrations from reducing environments at the bottom of the tuff at Yucca Mountain**

For purposes of estimating required critical mass (or radius) the nominal value of the uranium concentration which could be precipitated by an organic reducing zone beneath the repository could be conservatively estimated by the maximum concentration of uranium in the logs of the Colorado Plateau, which has been given in Section 7.4.3 as 20%. However, as an extra measure of conservatism, the MCNP analyses will be conducted over a range of values from this maximum to the worldwide peak concentration observed at Oklo, 60%.

#### **7.5 Minimum critical mass/radius at Yucca Mountain**

The critical mass calculation results presented in this section are described in detail in Ref. 5.43.

A set of 10 uranium/water concentrations in tuff was evaluated to determine the minimum critical mass/radius spheres. This set represented 3 SNF types, chosen to represent the 2%, 4%, and 13% most stressing fuel with respect to fissile content. For each of these fuel types, the analysis was a two step process. First the most critical volume %  $UO_2$  (highest  $k_{\infty}$ ) was determined for a family of water concentrations calculating  $k_{\infty}$  using MCNP, for a range of  $UO_2$  volume %. The  $k_{\infty}$  values for one fuel type (PWR, 3% initial enrichment, 20 GWd/MTU) are shown in



Figure 7.5-1. [It should be noted that the water concentrations in this figure are expressed as a volume percent of the tuff water mixture without uranium (for convenience of analysis in Ref. 5.43 from which the figure is taken), while the  $\text{UO}_2$  concentrations are expressed as a volume percent of the total rock (including the  $\text{UO}_2$ ).]

The second step is to calculate the  $k_{\text{eff}}$ , again using MCNP, for a range of radii, and interpolate to determine the critical radius, at which the value of  $k_{\text{eff}}$  is equal to the criticality threshold. The most appropriate value of criticality threshold  $k_{\text{eff}}$  was 1- (bias and uncertainty of the computational process) - (twice standard deviation of the specific Monte Carlo calculation). For these cases, the bias and uncertainty is lower than the usual value because it refers to the fissile content only. This is because we have made the *conservative assumption that none of the neutron absorbers from the SNF are in the uranium-bearing groundwater from the repository*, either having been removed from the SNF matrix much earlier than the fissile nuclides, or having remained in the matrix after removal of the fissile material. This process is illustrated in Figure 7.5-2, for the  $\text{UO}_2$  concentration giving the highest peak  $k_{\infty}$  for the family of water concentrations in Figure 7.5-1. Both figures are from Ref. 5.43.

The details of the calculations are given in Ref. 5.43. The results are summarized by the following table.

Table 7.5-1 Representative SNF/environment configurations and resulting spherical critical masses

SNF enrich & burnup (GWd/MTU)	Fissile % of SNF**	UO <sub>2</sub> vol % in rock*	H <sub>2</sub> O vol % in rock*	UO <sub>2</sub> wt % in rock†	H <sub>2</sub> O wt % in rock	Critical mass (MTU)*
3%, 20	1.94	18.5	38.3	58	11	1.6
3%, 20	1.94	8	43.2	35	17	10.1
3%, 20	1.94	17	33.2	54	9.6	2.50
3%, 20	1.94	8	36.8	33	14	10.1
3%, 20	1.94	15	25.5	48	7.5	6.5
3%, 20	1.94	10	27.0	37	9.1	7.4
3%, 20	1.94	8	27.6	32	10	18.0
3%, 20	1.94	11.6	17.7	39	5.5	55.2
3.5%, 30	1.87	14	25.8	46	7.8	11.1
4.0%, 40	1.82	15	25.5	48	7.5	30.9

\* These values correspond to those given in Ref. 5.43, Section 8.

\*\* These values are higher than those which would be computed from table 4.1-1, and which were used in Section 7.3, because they were derived under worst case reactor burn conditions, as contrasted with average reactor burn conditions used to develop the CDB data.

† The UO<sub>2</sub> wt % is computed from the volume percents by the formula  $10.96U_{v\%}/(10.96U_{v\%} + W_{v\%} + 2.52T_{v\%})$ , and the water wt% in a similar manner, where U<sub>v%</sub> is the volume percent of UO<sub>2</sub>, W<sub>v%</sub> is the volume percent of water and T<sub>v%</sub> is the volume percent of tuff.

## Far-Field External Criticality Analysis

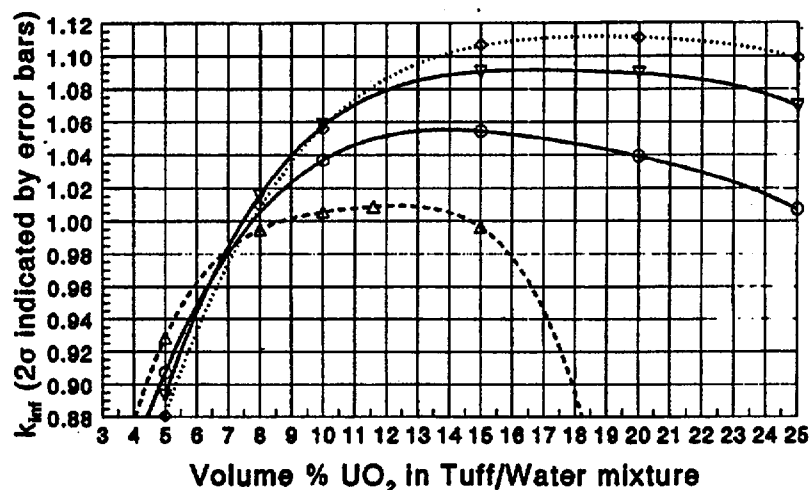
3.0% / 20 GWD/MT  $\text{UO}_2$  in Tuff/Water○ 38  $\text{H}_2\text{O}$ △ 20%  $\text{H}_2\text{O}$ ◇ 47%  $\text{H}_2\text{O}$ ▽ 40%  $\text{H}_2\text{O}$ 

FIGURE 7.5-1

Note: Error bars were not plotted if the  $2\sigma$  value was smaller than the data point marker.

## Far-Field External Criticality Analysis

3.0% Enriched, 20 GWD/MT, 18.5 vol%  $\text{UO}$ 

+ 47% Water in Tuff

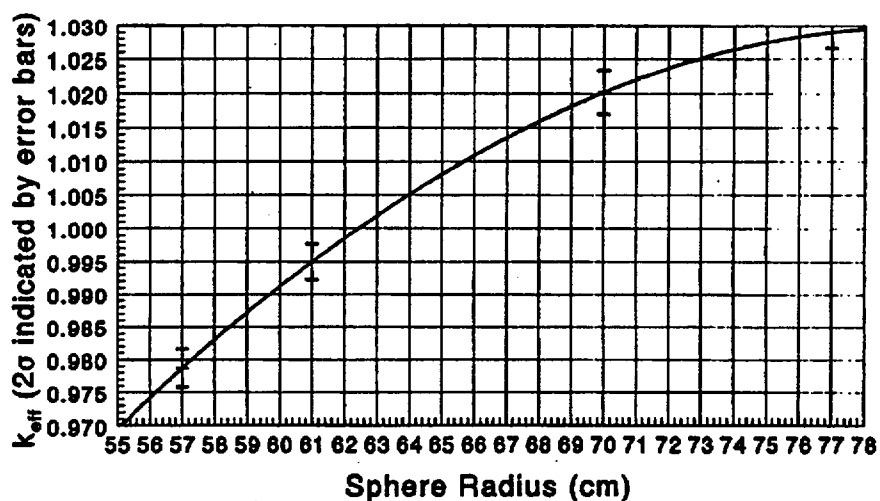


FIGURE 7.5-2

## **7.6 Upper bound on the Probability of Assembling a Critical Mass**

The methodology described in this section is based on the *assumption that the mass provided by a single log will be insufficient for criticality*. The validity of this assumption is demonstrated in Section 7.6.2, below. Because of this insufficiency, any reducing zone capable of adsorbing a critical mass will have to be built from a juxtaposition of logs.

### **7.6.1 Methodology**

The upper bound for the probability of the groundwater from a single waste package precipitating into a critical mass is determined by combining two independent probabilities, according to the following formula

$$\text{Pr}\{\text{critical precip per pkg}\} = \text{Pr}\{\text{log}\} * \text{Pr}\{\text{cluster}|\text{log}\},$$

where  $\text{Pr}\{\text{log}\}$  is the probability of the repository effluent encountering a carbonized log, and  $\text{Pr}\{\text{cluster}|\text{log}\}$  is the probability that the log is part of a cluster of sufficient size to precipitate a critical mass. The required cluster size, or mass, is inversely proportional to the fissile content of the fuel in the waste package which served as the source of the groundwater flow, and is also inversely proportional to the uranium and water concentrations, as indicated in the results of the previous section (Table 7.5-1).

The total probability of criticality is obtained by multiplying  $\text{Pr}\{\text{critical precip per pkg}\}$  by the number of waste packages having sufficient fissile percentage to produce a criticality with the cluster size associated with the corresponding  $\text{Pr}\{\text{cluster}|\text{log}\}$ .

The next two sections describe the computation of  $\text{Pr}\{\text{cluster}|\text{log}\}$  and of  $\text{Pr}\{\text{log}\}$ .

### **7.6.2 Probability of reducing material, $\text{Pr}\{\text{cluster}|\text{log}\}$**

This section is a summary of the data analysis and calculations described in Attachment II.

The concentrations of uranium required for criticality can be modeled by the juxtaposition of logs onto a circle through the cross section of the critical mass sphere, to achieve the specified critical mass (upwards of 1 metric ton  $\text{UO}_2$ ). The probability of such random juxtapositions is built from the probability distributions of log length and of uranium concentration within the log.

In this model, three log parameters are generated from specific distributions: log

length, potential concentration of uranium, and log radius. For the distribution of log lengths, the analysis of Attachment III shows a negative exponential distribution with a floor of 3.0 meters and a decay length of 4.6 meters.

Based on analysis of 3 data sources in Attachment II, a uniform distribution between 1% and 21.5% is used for potential uranium concentration

$$f_o(x) = 1/(x_2 - x_1) \quad \text{for } x_1 < x < x_2$$

where  $x$  is expressed as a fraction (instead of a percent) to correspond to the actual mathematics of calculation used in the program listing below, and the constant values are  $x_1 = 0.01$ ,  $x_2 = 0.215$ . This distribution gives an average ore grade ( $U_3O_8$  concentration) of 11.25%.

It should be noted that for the highest concentration in this distribution, 21.5wt% (4.3 vol% assuming 47 vol% water in the remaining rock, or 4.6 vol% assuming 40 vol% water in the remaining rock),  $k_{\infty} < 0.9$ , as can be seen from Figure 7.5-1, so there is no possibility of criticality of any size log of this concentration. It is still necessary, however, to consider the juxtaposition of logs as representing the possibility of higher concentrations, even though no single log could reach such high concentrations. The juxtaposition of material presumes the organic material in multiple logs is chemically concentrated. The concentration of organic material provides a concentrated reducing zone with the capability of producing uranium concentrations higher than possible with individual logs.

Although no geological analogs for such an organic reducing zone concentration process exist in the United States, it is thought that some highly concentrated organic reducing zone was responsible for the highest uranium concentrations observed at Oklo (up to 60%, Ref. 5.34, p. 20). In the absence of a geochemical model of the transformations which would be required for such a concentration process, the probabilistic/analog analysis is offered as a very conservative estimate of the actual risk. The probabilities of occurrence of the actual physical and chemical processes are currently unknown. Because of the lack of direct observations of the actual occurrence of such processes, any associated probabilities are assumed to be quite small.

For the distribution of log radii, the smallest of 4 diameters cited by Hess (Ref 5.29, pg 467), 16 inches, which translates into a radius of 20 cm, is used as the lower limit. The distribution is taken to be triangular with peak at this lower limit, based on anecdotal information from those who have seen the logs (e.g. Ref. 5.41) and the assumption that only the few largest logs are of sufficient interest to be reported in the literature. Since the probability density of a triangular decreases to zero at the upper limit, this upper limit is taken to be well above radius

corresponding to the maximum observed diameter, 4 feet (61 cm radius) given by Hess. This distribution is a conservative model because the Hess article is primarily interested in reporting the largest ore concentrations, which would correspond to the largest logs. This conservative designation for the model is also consistent with the Chenoweth (Ref. 5.15, pg 166) statement cited above that the largest log diameter is 1 meter. The pdf for the resulting triangular distribution is

$$f_r(r) = 2(rl_2 - r)/(rl_2 - rl_1)^2 \quad \text{for } rl_1 < r < rl_2$$

where  $rl_1 = 0.20$  meter,  $rl_2 = 0.80$  meter.

As a worst case, the potential for criticality of the largest log can be estimated under the further conservative approximation that it contain the maximum possible uranium concentration, 21.5 wt%. It was already shown, above, that  $k_{\infty} < 0.9$ ; however, it is of interest to evaluate  $k_{\text{eff}}$  for this case. For 4.6 vol%  $\text{UO}_2$ , with the remaining rock being 40 vol% water and 60 vol% tuff,  $k_{\text{eff}} = 0.79$  (Ref. 5.43).

The methodology can now be summarized by an algorithm stated as follows: (1) Determine a critical mass - critical radius pair from the set generated in Ref. 5.43, and apply the adjustment factors 0.325 and 0.686, respectively, as a measure of conservatism to account for the neutron contribution of the portions of the logs falling outside the critical sphere; (2) Select the three random parameters for a sample log from the appropriate distributions as described above (log length, log radius, uranium wt%); (3) Calculate the contributed mass for this log from Eq (2), above and accumulate the sum of the masses of overlapping logs thus far; (4) Multiply the accumulated probability by the value for this log as computed from Eq (1) of Attachment II, using the uncorrected sphere radius; (5) If the accumulated mass is greater than the required critical mass, end the calculation and report the remaining probability, otherwise repeat steps (2) through (5) for the next log. This algorithm is repeated, starting with step 1, for each critical mass - critical radius pair in the set generated in Ref. 5.43.

**Table 7.6-1 Upper bound of probabilities of log clusters which could be capable of precipitating a uranium concentration sufficient for criticality**

<b>Fissile %</b>	<b>UO<sub>2</sub> g/cm<sup>3</sup></b>	<b>H<sub>2</sub>O g/cm<sup>3</sup> *</b>	<b>Critical radius (m) †</b>	<b>Critical mass (metric ton) †</b>	<b>Pr{cluster log} ‡</b>
1.94	2.03	0.383	0.394	0.520	1.58x10 <sup>-4</sup>
1.94	0.877	0.432	0.961	3.283	3.71x10 <sup>-14</sup>
1.94	1.86	0.332	0.470	0.813	9.63x10 <sup>-7</sup>
1.94	0.877	0.368	0.961	3.283	8.31x10 <sup>-11</sup>
1.94	1.64	0.255	0.673	2.112	1.52x10 <sup>-11</sup>
1.94	1.10	0.270	0.803	2.405	1.43x10 <sup>-10</sup>
1.94	0.877	0.276	1.167	5.850	1.52x10 <sup>-21</sup>
1.94	1.27	0.177	1.496	17.940	1.03x10 <sup>-57</sup>
1.87	1.53	0.258	0.824	3.608	4.7x10 <sup>-18</sup>
1.82	1.64	.255	1.133	10.042	7.18x10 <sup>-48</sup>

\* This column is simply the vol% water of Table 7.5-1 divided by 100.

† These columns computed in Attachment II as adjustments from the values in Ref. 5.43. The critical mass is, therefore, adjusted from the values given in Table 7.5-1

‡ The arithmetic means from Attachment II have been used for conservatism.

### **7.6.3 Probability of encountering a log, Pr{log}**

The calculations of this section are based on the possible analogy between the planar distribution of logs observed on the Colorado Plateau and logs which could be distributed somewhere at the base of the tuff beneath Yucca Mountain.

Since there are no statistics on logs at the base of the ash-flow tuff of Yucca Mountain, there is no direct way to estimate Pr{log}. A very conservative upper bound can, however, be developed from statistics of the log occurrences on the Colorado Plateau, according to the formula

$$\text{Pr}\{\text{log}\} = (\text{Area occupied by logs})/(\text{Area of sample space}),$$

where the sample space is the area which has been investigated for logs. The analysis starts with the 84 logs counted in the 87,000 m<sup>2</sup> orebody described by Fischer (Ref. 5.28). Using the triangular distribution of log radii given above, the

average radius can be calculated as 40 cm so that the average diameter is 80 cm. Using the negative exponential distribution of log lengths given above, an average of 7.6 meters is calculated. The total cross-section area of 84 logs lying horizontally is 511 m<sup>2</sup>. The question is what larger area (or sample space) this represents.

Chenoweth (Ref 5.41) has estimated that the geologic formation of the Colorado Plateau in which the logs are found occupies 1100 square miles (2850 km<sup>2</sup>). He has also estimated that there are 165 orebodies similar to the one mapped by Fischer in this area. Since these orebodies have not been mapped for log occurrences, the best estimate of the total log area in this 2850 km<sup>2</sup> sample space would be to simply multiply the 511 m<sup>2</sup> of the Fischer orebody by 165, giving a total log area of 84,000 m<sup>2</sup>. *This analysis is equivalent to the assumption that the sample space for the distribution of organic deposits (to be found at the base of the tuff under Yucca Mountain) is the entire geologic formation containing log deposits in orebodies on the Colorado Plateau.*

An alternative, and more conservative, interpretation would be that the identified orebodies do not represent all the occurrences of logs, only those which would be mineralized. To be mineralized, the organic log must not only exist, it must also be contacted by a uranium-bearing groundwater. Since there is no way to estimate the number of unmineralized logs in the large sample space identified by Chenoweth, the alternative is to use a smaller sample space. This can be defined by examining a map of orebodies in a buried river channel given in Thamm et. al. (Ref 5.31, p. 50) which shows the orebodies to be occupying approximately 7% of the riverbed. Since the entire river channel was probably exposed to the same uranium-bearing groundwater, all identified orebodies should represent all the organic matter present. Hence the area of this smaller, more conservative, sample space could be estimated by dividing the area of the orebody by .07. *This analysis is equivalent to the assumption that the sample space for the distribution of organic deposits (to be found at the base of the tuff under Yucca Mountain) is a typical buried river channel found on the Colorado Plateau and diagrammed in Ref. 5.31, and that such a buried river channel exists at the base of the tuff beneath Yucca Mountain.*



The results for the two alternative interpretations are given in the following table.

Table 7.6-2 Alternative estimations of probability of encountering a log

Sample Space	Area of sample space (km <sup>2</sup> )	Total log area in sample space (m <sup>2</sup> )	Pr{log}
Underground river channel	1.24*	511	$4.1 \times 10^{-4}$
Geologic formation	2850	84,000	$2.9 \times 10^{-5}$

\* Calculated from Ref 5.31, figure 16.

#### 7.6.4 Calculation of expected number of criticalities

The expected number of criticalities is the product of three factors:

- The number of waste packages with sufficient fissile content to provide a source for a reducing zone
- The probability of the stream from a single waste package encountering a reducing zone, Pr{log}
- The probability of the reducing being of sufficient size to remove a critical mass, Pr{cluster|log}

The number of waste packages for each criticality threshold is determined from the tabulation of percentiles of number of PWR assemblies having greater than a specified  $k_{inf}$  given in Ref. 5.10, where the  $k_{inf}$  is calculated as a function of enrichment and burnup according to the procedure also given in that reference. The results are given in the following table.

Table 7.6-3 Percentile of SNF having less fissile % than stated value

% enrichment, burnup (GWd/MTU)	% Fissile	$k_{inf}$	Fissile content percentile
3.0%, 20	1.94	1.13	98
3.5%, 30	1.87	1.08	96
4.0%, 40	1.82	1.04	87

Using the expected total of 12,000 waste packages of commercial SNF (Ref. 5.49), and making the conservative *assumption that the packages are loaded homogeneously (so that all the high fissile fuel is grouped together)*, the number of packages having higher fissile content (or higher  $k_{inf}$ ) than the indicated values can be estimated by multiplying the total number of waste packages by the complement

of the percentile in the above table, and dividing by 100.

For  $\text{Pr}\{\log\}$  the conservative alternative from Table 7.6-2,  $4.1 \times 10^{-4}$  is used. For  $\text{Pr}\{\text{cluster}|\log\}$  the values from Table 7.6-1 are used, except that the cases which require a high volume % water should have the probabilities of Table 7.6-1 multiplied by the probability of finding such a high porosity in the saturated zone. From Table 7.5-1 it is seen that the first 4 cases all require more than 30 vol% water (which is equivalent to porosity in the saturated zone). From Table 7.6-1 it is seen that the first and third cases will be the only ones contributing significantly to total probability. These cases require 38.3 and 33.2 percent porosity, respectively. From Figure 4.1-1 it is seen that the probabilities of having such high porosities are .01 and .23, respectively. Multiplying by the corresponding probabilities in Table 7.6-1 and adding gives  $1.8 \times 10^{-6}$  for the porosity adjusted  $\text{Pr}\{\text{cluster}|\log\}$ .

Although only the first and third cases of Table 7.6-1 can contribute significantly to the overall expected number of criticalities, it is still useful to present the results for the last 2 cases which represent different fuel characteristics, and a lower fissile content. These cases do not need to be porosity adjusted because they have porosities of less than 26%, which can be found in over 90% of the rock.

Table 7.6-4 Summary of upper bound for probability of criticality as a function of fissile content

% fissile	Number pkgs with more fissile	$\text{Pr}\{\text{cluster} \log\}$	Expected criticalities
1.94*	240	$1.8 \times 10^{-6}$ **	$1.8 \times 10^{-7}$
1.87*	480	$4.70 \times 10^{-18}$ *	$9.2 \times 10^{-19}$
1.82*	1560	$7.18 \times 10^{-48}$ *	$4.6 \times 10^{-48}$

\* From Table 7.6-1

\*\* Porosity adjusted as described above

#### 7.6.5 Adjustment for critical masses greater than a single waste package

For those cases with required critical mass significantly greater than 10 tons (the contents of 1 waste package) some focusing from 2 or more waste packages would be necessary. There are two mechanisms for such focusing: (1) Random fractures which accidentally happen to channel the flow in a concentrating direction, and (2) highly permeable rock which acts as an attractor for groundwater streamlines. This section provides a simplified analysis of the first mechanism. It should be noted that this section stands alone, and is for illustrative purposes only, so that if future investigations indicate a significant potential for the second mechanism, the validity of other sections of this document will not be affected, and

the conclusions will remain unchanged.

which would decrease the probability by multiplying by a factor less than the ratio of the critical sphere cross section area divided by the repository area enclosing the required number of waste packages, which could be quite a small factor if the design basis waste packages are distributed throughout the repository. There are four cases in Table 7.5-1 which require significantly more than 10 tons of uranium, but this correction has not been applied because the initial calculation showed the probability to be incredibly small. It should be noted that groundwater focusing does occur naturally, but rarely, as the source of artesian springs being at the focus of a large catchment area.

It is, nevertheless, useful to estimate the per-package multiplicative factor. At 80 MTU/acre, the average area per waste package is 493 sq meters; a typical critical sphere radius from Table 7.6-1 is 1 meter, so the reduction factor would be  $\pi/493 = 0.006$ .

It should be noted that a realistic analysis of the groundwater flow in the saturated zone from a single waste package indicates a dilution of such magnitude that even the smallest critical mass requirements of Table 7.6-1 would require more than one package. The following simplified analysis indicates the magnitude of the dispersion.

It is conservatively *assumed that the groundwater which has passed through a waste package flows vertically downward through the unsaturated zone with no lateral dispersion*. In the saturated zone the flow follows the fluid potential gradient with a dispersion approximated by Equation 7.6-5 of Ref 5.18 which gives the concentration as a function of vertical distance below the water table,  $z$ , distance from the plume centerline,  $y$ , and downstream distance,  $x$ ,

$$C(x,y,z) = (2Q/u) \exp\{-y^2/[4D_y(x/u)] - z^2/[4D_z(x/u)]\} / [4\pi\phi(D_y D_z)^{.5}(x/u)],$$

where  $Q$  is the mass flux from a point source,  $u$  is the groundwater velocity,  $\phi$  is the porosity, and  $D_y$  and  $D_z$  are the diffusion coefficients in the  $y$  and  $z$  directions and are modeled by

$$D_y = \beta_y x u, \quad D_z = \beta_z x u$$

*Conservatively assuming  $y=0$ , the concentration will peak at a downstream distance of  $x = z^2 \text{sqrt}(1/\beta_z)/2$ .*

The remaining parameters are modeled as follows:

$\phi = V_{\text{sat}}/u$ ,  $Q = C_{\text{uz}}V_{\text{uz}}A$ , where  $A$  is the waste package footprint, and the subscripts indicate the zone to which the parameters apply, which reduces the concentration formula to

$$C/C_{\text{uz}} = 4V_{\text{uz}}A\text{sqrt}(\beta_z/\beta_y)\exp(-1)/[V_{\text{sat}}z^2]$$

Generally,  $V_{\text{uz}} < V_{\text{sat}}$ ,  $\beta_z/\beta_y < 0.1$ , and for any appreciable distance below the water table  $A \ll z^2$ , so the concentration of uranium from a waste package will be diluted by at least a few orders of magnitude by the time it has moved a few hundred meters below the water table (top of the saturated zone).

Since the smallest critical mass found in this study is 16% of a waste package (1.6 tons required for the smallest critical mass out of approximately 10 tons uranium in the whole waste package), this dilution implies that the streams from a number of waste packages would have to be combined to deposit a single critical mass. Since the probabilities calculated without this correction are already very small, the correction was not quantified further or applied.

### **7.7 Increase in radionuclide inventory**

This section provides a conservative estimate of the maximum possible increase in radionuclide inventory which could result from an external criticality, in the very unlikely event that such a criticality did occur. The estimate is based only on a worst case geologic analog, since there is insufficient information on the range of specific parameters of such a reactor to enable the use of a reactor depletion code. The simplified analysis of this section is for illustrative purposes only, and any question regarding its assumptions or methods should not effect any other sections of this document or the conclusions.

The increase in radionuclide inventory due to a criticality is generally proportional to the burnup. This, in turn, is generally proportional to the reduction in fissile content. For an external criticality the reduction in fissile content will be shown below to be conservatively bounded by the difference between 1.94% and 1.37%. The Oklo reactors existed  $\approx 2$  billion years ago, at which time the natural enrichment would have been 3.68% (Ref. 5.34, p. 20). What is now observed as the present minimum enrichment of 0.265% (depleted with respect to the present normal 0.711%), would have been  $(3.68\%/0.711\%)*0.265\% = 1.37\%$  at 2 billion years ago. It is assumed that an external criticality which could be started with the 1.94% fissile content of the highest 2% of commercial SNF would burn down no further than a fissile content of 1.37%. This is an extremely conservative assumption, since Table 7.5-1 shows very large critical mass required for fissile content as high as 1.82%, indicating that a criticality in the Yucca Mountain environment could not be sustained for a fissile content much below that number.

*It is assumed that the increment of burnup provided by the external criticality is proportional to the reduction in fissile content of the fuel.* The maximum reduction in fissile content for the presumed external criticality is 1.94-1.37, which compares with the reduction in fissile content to produce the 3%, 20GWd/MTU SNF in the first place (3.00-1.94). The ratio of external criticality burnup to initial in-reactor burnup is  $0.57/1.06 = .54$ , or 54%. This is much larger than the 4% burnup increment for a waste package criticality found in Ref. 5.50, because that SNF reactor duration was limited by the expected maximum period of increased infiltration rate (10,000 years), whereas in the saturated zone the increased water concentration can be presumed to last indefinitely, with the principal shutoff mechanism being depletion of fissile material or buildup of neutron absorbers.

*It is further assumed that the increase in radionuclide inventory is proportional to the increment of burnup.* From Table 7.6-4 it is seen that the design basis fuel (1.94% fissile content) has by far the largest contribution to expected number of criticalities. Since this first line of the table represents only 2% of the waste packages, and since any criticality can only increase the already existing radionuclide inventory of an individual waste package by 54%, the total radionuclide inventory in the repository can only be increased by 1% (54% of 2%). When multiplied by the very small probability of this event in the first place, the contribution to radionuclide inventory risk is negligible.

### **7.8 Possibility of autocatalytic criticality**

Autocatalytic criticality is broadly defined to include any increase in  $k_{eff}$  as water is driven from a critical mass. To determine the circumstances under which this can occur,  $k_{eff}$  is calculated for a sequence of configurations having the same fissile concentration and the same porosity, but with decreasing percentages of water in the porespace.

Autocatalytic criticality can occur in an overmoderated system. Overmoderation occurs when the concentration is far in excess of the amount needed as moderator to thermalize the neutron spectrum. Once the moderator increases beyond what is strictly necessary to slow down most of the neutrons to thermal, any additional moderator will produce no reactivity increasing benefit. In fact, if the moderator is also a neutron absorber, like water, then an increase in concentration beyond the point of optimum moderation will reduce  $k_{eff}$ . The corollary to this behavior is that in an overmoderated condition the removal of water may increase  $k_{eff}$ .

The possibility of autocatalytic criticality for highly enriched fissile material (plutonium or highly enriched uranium, HEU) has been suggested by Bowman (Ref 5.35) and verified by Kastenberget al.(Ref 5.4). This section will show that any

autocatalytic criticality which did occur in commercial SNF would be very weak, because of the low fissile content (very low enriched uranium, VLEU).

To examine the question of autocatalytic criticality for VLEU,  $k_{\text{eff}}$  is calculated for a sequence of water concentrations in a rock having 8%, by volume, of  $\text{UO}_2$  resulting from the decay ( $^{239}\text{Pu}$  to  $^{235}\text{U}$ ) of SNF having a burnup of 20 GWd/MTU, and having had an initial enrichment of 3%. The rock also has a voidspace (fractures plus pores) of 43.2%, with the remaining 48.8% being typical of the tuff beneath Yucca Mountain. These conditions were chosen because they are representative of the most stressing with respect to criticality.

Starting with the voidspace fully occupied by water, a sequence of steps reduces the water concentration while maintaining the same voidspace, uranium concentration, and tuff. The resulting  $k_{\infty}$  and  $k_{\text{eff}}$  (for a 150 cm radius sphere) curves as a function of water concentration are shown in Figure 7.8-1; the details of these calculations are provided in Ref. 5.43.

From this figure, it is seen that, starting from the highest water concentration, decreasing the water will increase  $k$  until a peak is reached, beyond which continued decrease of water concentration will be loss of vitally needed moderator, and its loss will reduce  $k$  (both  $k_{\text{eff}}$  and  $k_{\infty}$ ). As would be expected, the effect is much stronger for  $k_{\infty}$  than for  $k_{\text{eff}}$ . However, the practical effect of such a limited autocatalytic criticality is likely to be insignificant for the following reasons:

- Any power pulse which could rapidly reduce the water concentration would be likely to carry the reduction beyond the peak to the positive sloping region where continued water loss will reduce  $k_{\text{eff}}$ , and shut the reaction down.
- The 150 cm sphere shows only a very weak effect which would hardly exist if the threshold for criticality were  $k_{\text{eff}} = 1$ , rather than the lower value, 0.985 which is used to reflect bias and uncertainty.

The very limited autocatalytic criticality shown in Figure 7.8-1 differs from the stronger effect shown in Kastenberg et. al. (Ref 5.4) primarily because of the lower enrichment, or fissile content. In fact if the curves for the change in  $k_{\infty}$  of figure 3 of Ref 5.4 are projected to the .02 enrichment level, they cross the  $k_{\infty} = 1$  line so there would be no effect at all. The only reason that Figure 7.8-1 shows an autocatalytic criticality effect at all is that it starts with a very high porespace, or water concentration, of 0.43 g/cm<sup>3</sup>. By comparison, Figure 3 of Ref. 5.4 shows only curves for initial water concentrations of 0.1 g/cm<sup>3</sup> and 0.2 g/cm<sup>3</sup>; if the trend of increasing  $k_{\infty}$  with increasing initial water density were continued, a curve for 0.43 g/cm<sup>3</sup> using the Kastenberg methodology would show the effect seen in Figure 7.8-1 of this document.

## Far-Field External Criticality Analysis

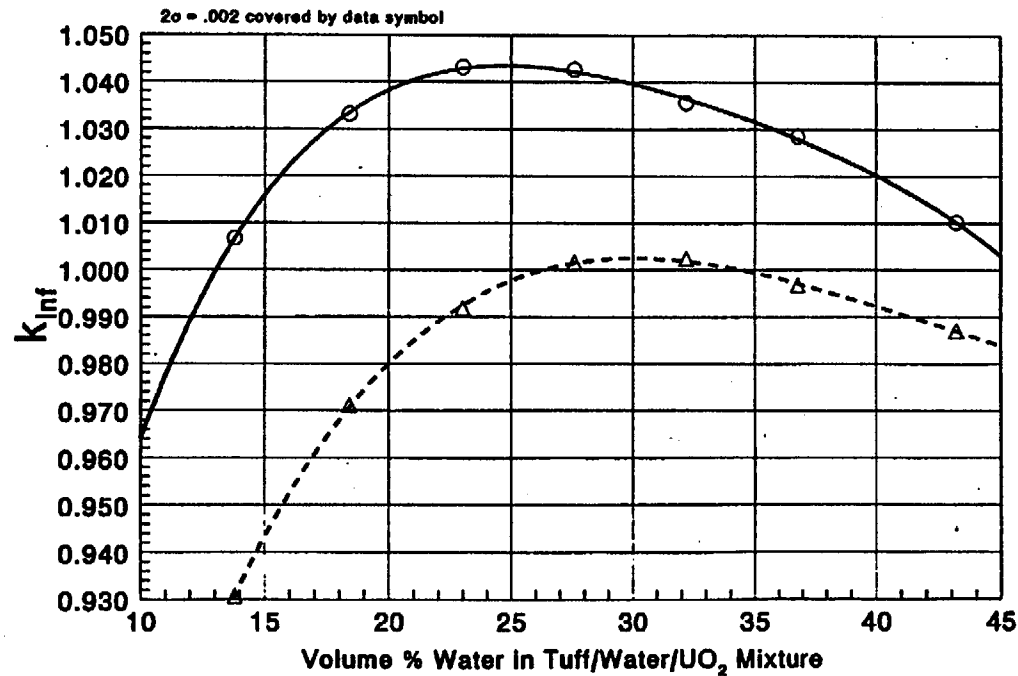
3.0%/ 20 GWD/mt  $\text{UO}_2$  in Tuff/Water Mixture (Porosity=0.47)○ 8.0%  $\text{UO}_2$ , Infinite△ 8.0%  $\text{UO}_2$ , 150 cm Radius Sphere

FIGURE 7.8-1

## **8. Conclusions**

In compliance with the M&O Quality Administrative Procedures, the design results presented in this document should not be used for procurement, fabrication, or construction unless properly identified, tracked as TBV, and controlled by the appropriate procedures.

The purpose of this analysis was to evaluate the criticality potential of the repository far-field environment when contacted by a uranium-bearing groundwater stream. As a result of the calculations performed in this analysis, it can be concluded that:

- The only feasible mechanism for concentrating a critical mass of commercial SNF uranium is for uranium-bearing groundwater to contact a reducing zone of significant size; the strongest reducing zones for the concentration of uranium have been the accumulation of organic material; the only place in the tuff beneath Yucca Mountain where such an accumulation of organic material could occur is at the base of the tuff.
- The probability of collecting a local concentration of organic material large enough to precipitate a critical mass of VLEU is very small.
- While there is significant potential for adsorption of uranium from groundwater by zeolites of the type found in abundance at Yucca Mountain, the maximum concentration achievable from such adsorption would be far below that necessary for criticality in commercial SNF. Furthermore, it can be concluded that the extensive zeolite layers will remove a major fraction of the uranium from any groundwater stream from the repository, thereby reducing the amount of uranium reaching any organic reducing zones and providing an additional measure of conservatism for the evaluation of those reducing zones given in this document.
- This study has been unable to identify any other mechanisms for uranium concentration which could possibly produce a high enough concentration to produce criticality in commercial SNF. It is unlikely that such a mechanism will be found, since there is only one known natural concentration of uranium which is sufficiently high to produce criticality (60% at Oklo).
- There is a possibility of autocatalytic criticality (positive feedback) from overmoderation, in the very low probability that such a criticality could occur in the first place. However, the high water concentration required is very unlikely, and if such a autocatalytic criticality did occur, the system would quickly lose enough water to move into a negative feedback regime and shut down the criticality.



From the results of this analysis it is recommended that future studies should:

- Determine the geochemistry of the invert and analyze the potential for precipitation of a critical mass.
- Perform an in-depth screening of geochemical processes and geologic scenarios to identify any which could produce a sufficiently concentrated reducing zone in tuff (either organic or otherwise) to precipitate a critical mass of commercial SNF uranium (VLEU).
- Evaluate the potential for external criticality for highly enriched DOE owned SNF.

**9. Attachments -**

**List of Attachments**

<u>Attachment</u>	<u>Description</u>	<u>Date</u>	<u>Number of Pgs</u>
I	Details of the Decay/Removal Calculation	5/28/96	14
II	Upper bound on the probability of formation of a reducing zone capable of collecting a critical mass	5/28/96	18
III	Statistics for fossil logs found in the Club Group of Mines, Montrose County, CO	5/31/96	9
IV	WP AUCF Design Inner Barrier (21 PWR) Engineering Sketch	5/31/96	1

**Details of the decay/removal calculation**

This attachment consists of three programs with source code, input file, and output file for each. These programs simplify the SNF components to three isotopes of greatest concern for long-term external criticality:  $^{239}\text{Pu}$ ,  $^{235}\text{U}$ , and  $^{238}\text{U}$ , and compute the remaining amounts of each as a function of time for a range of removal rate process parameters. The programs also include the decay of  $^{239}\text{Pu}$  into  $^{235}\text{U}$ . These programs provide the details of the calculations summarized in Section 7.3 of the main document.

The following program is used for the cases of approximation A of Section 7.3.

Source Code "c:\temp\richstat.c" 5/23/96

```
/* richstat.c Program to remove fissile material from SNF in a waste
package while decaying the Pu239 to U235. Program reads input
of 6 parameters per line/case (max ppm U, max ppm Pu, mm/yr infiltration,
initial kg U235, initial kg Pu239, initial kg U238) from the
input file "richstat.in" until the file is exhausted. For each case
the components U238, U235, and Pu239 are decremented until one of them
is exhausted. This program also does the following:
(1) Determines the maximum and minimum
effective fissile percent and prints the concentrations and time at
which the maximum and minimum occur; (2) Prints a set of halfway
statistics when the fissile content is half the initial value, if
such a condition occurs before one of the nuclide species is exhausted.
In addition to these special points, the program prints the starting
and ending values of concentration and effective enrichment. This
version of the program accounts Pu239 the same as U235. An alternate
version (richsta.c) implements a factor of 1.25 multiplying the
Pu239 concentration to account for the extra neutron efficiency which
can occur under some circumstances.*/
```

```
#include <stdio.h>
#include <stdlib.h>
```

```
void main()
{int year, //Counts time in intervals of 1000 years
 yearmax, yearmin, //Times (in 1000 years) of max and min eenr occur
 yearhalf, //Year at which the fissile content is half the starting value
 foundhalf; //Indicator of whether a half fissile has occurred by the time
 //one of the species is depleted, for this case.
float mu238, //Current mass of U238 kg (decremented at each iteration)
 mu235, //Current mass of U235
 oldmu235, //Temporary value for consistency in updating
 mp239, //Current mass of Pu239
 maxu, maxp, //Solubilities of U and Pu, ppm
 infl, //Infiltration rate, mm/yr.
```

```

pkgarea=6.46, //Horizontal cross section in sq meters
volflow, //Vertical volumetric flow rate through a waste package, m3/yr.
pdr=1/24.4, //Pu decay rate, per 1000 yrs
fissile, //Plutonium plus U235
mtotal, //Total of all three isotopes (fissile+U238)
eenr, //Effective enrichment (fissile/mtotal)
eenrmax, pumax, u238max, u235max, //maximum effective enrichment and
//associated mass parameters
eenrmin, pumin, u238min, u235min, //minimum effective enrichment and
//associated mass parameters
eenrhalf, puhalf, u238half, u235half, //parameters associated with the
//50% fissile depletion point
eenrstart, pustart, u238start, u235start, //Initial values
FILE *fin, *fout;
fin=fopen("richstat.in", "r");
fout=fopen("richstat.out", "w");
while(fscanf(fin, "%f %f %f %f %f",
    &maxu, &maxp, &infl, &mu235, &mp239, &mu238) != EOF) //read parameters and
    //initial values for this case
{
    volflow=infl*pkgarea*.001; //compute volumetric flow m3/yr
    fprintf(fout, "\n\nMax U ppm=%8.3f  Max P ppm=%8.3f  mm/yr=%7.1f\n",
        maxu, maxp, infl); //print parameter value header for this case
    fprintf(fout, "%6s%12s%12s%12s\n", "Time", "U238 kg", "U235 kg",
        "Pu239 kg", "eff enrch"); //print column headings for this case
    year=0; //Initialize starting time for this case
    foundhalf=0; //Start with no halfway point for this case
    yearmax=yearmin=0; //Initialize max and min times to start
    pustart=pumax=pumin=mp239; //Initialize mass values to starting values
    u238start=u238max=u238min=mu238;
    u235start=u235max=u235min=mu235;
    fissile=mu235+mp239; //compute initial fissile
    mtotal=fissile+mu238; //compute initial total mass
    eenrstart=fissile/mtotal; //compute initial effective enrichment
    eenrmax=eenrmin=eenrstart; //initialize max and min of eenr
    while((mu235>0) && (mp239>0)) //Loop until one of the fissile is depeleted
    {
        fissile=mu235+mp239; //Update fissile
        mtotal=fissile+mu238; //Update mtotal minus adjustment to fissile
        eenr=fissile/mtotal; //Update effective enrichment
        oldmu235=mu235; //Compute temporary mass for update consistency
        if(eenr>eenrmax) //Update maximum eenr point if appropriate
        {
            eenrmax=eenr;
            yearmax=year;
            u238max=mu238;
            u235max=mu235;
            pumax=mp239;
        }
        else if(eenr<eenrmin) //Update min eenr point if appropriate
        {
            eenrmin=eenr;
            yearmin=year;
            u238min=mu238;
        }
    }
}

```

```

    u235min=mu235;
    pumin=mp239;}
    if((foundhalf==0)&&(fissile<.5*(u235start+pustart)))
    {foundhalf=1;//Test for halfway point and update as appropriate
    yearhalf=year;
    puhalf=mp239;
    u235half=mu235;
    u238half=mu238;
    eenrhalf=eenr;}
//The next 3 lines are the basic updating equations for each iteration
mu235=mu235-volflow*maxu*mu235/(mu235+mu238)+pdr*mp239*235/239;
mp239-=pdr*mp239+volflow*maxp;
mu238-=volflow*maxu*mu238/(oldmu235+mu238);
year++;}
fprintf(fout,"%6d%12.3f%12.3f%12.3f%12.6f%12s\n",
    0,u238start,u235start,pustart,eenrstart,"Start");
fprintf(fout,"%6d%12.3f%12.3f%12.3f%12.6f%12s\n",
    yearmin,u238min,u235min,pumin,eenrmin,"Min");
if(foundhalf==1)fprintf(fout,"%6d%12.3f%12.3f%12.3f%12.6f%12s\n",
    yearhalf,u238half,u235half,puhalf,eenrhalf,"Half");
fprintf(fout,"%6d%12.3f%12.3f%12.3f%12.6f%12s\n",
    yearmax,u238max,u235max,pumax,eenrmax,"Max");
fprintf(fout,"%6d%12.3f%12.3f%12.3f%12.6f%12s\n",
    year,mu238,mu235,mp239,eenr,"End");}}

```

Input file "c:\temp\richstat.in" (with column headings added for clarity)

The run consists of 10 cases, the first 5 for the design basis fuel (3% initial enrichment and 20 Gwd/MTU), and the second five for 4% initial enrichment and 40 Gwd/MTU. The difference between the two fuel types is reflected by the different initial quantities of the 3 principal isotopes, mu235, mp239, mu238. The five cases for each fuel type differ by the maximum uranium solubility, maxu, which determines the uranium removal rate, since the removal process is solubility limited (also called flux limited). The column headings have been added for clarity; they are not present in the actual file.

maxu	maxp	infl	mu235	mp239	mu238
120	.12	10	126.8	44.2	9314.3
150	.12	10	126.8	44.2	9314.3
200	.12	10	126.8	44.2	9314.3
1200	.12	10	126.8	44.2	9314.3
2400	.12	10	126.8	44.2	9314.3
120	.12	10	94.4	61.8	8905
150	.12	10	94.4	61.8	8905
200	.12	10	94.4	61.8	8905
1200	.12	10	94.4	61.8	8905
2400	.12	10	94.4	61.8	8905

## Output file "C:\temp\richstat.out"

Max U ppm= 120.000		Max P ppm= 0.120		mm/yr= 10.0	
Time	U238 kg	U235 kg	Pu239 kg	eff enrch	
0	9314.300	126.800	44.200	0.018028	Start
130	8323.798	152.002	0.003	0.017934	Min
0	9314.300	126.800	44.200	0.018028	Max
131	8316.185	151.864	-0.004	0.017934	End

Max U ppm= 150.000		Max P ppm= 0.120		mm/yr= 10.0	
Time	U238 kg	U235 kg	Pu239 kg	eff enrch	
0	9314.300	126.800	44.200	0.018028	Start
130	8076.199	147.668	0.003	0.017956	Min
17	9151.986	146.474	21.604	0.018034	Max
131	8066.683	147.494	-0.004	0.017956	End

Max U ppm= 200.000		Max P ppm= 0.120		mm/yr= 10.0	
Time	U238 kg	U235 kg	Pu239 kg	eff enrch	
0	9314.300	126.800	44.200	0.018028	Start
130	7663.542	140.426	0.003	0.017995	Min
35	8869.135	153.056	10.072	0.018061	Max
131	7650.855	140.193	-0.004	0.017995	End

Max U ppm=1200.000		Max P ppm= 0.120		mm/yr= 10.0	
Time	U238 kg	U235 kg	Pu239 kg	eff enrch	
0	9314.300	126.800	44.200	0.018028	Start
0	9314.300	126.800	44.200	0.018028	Min
65	4360.086	82.491	2.735	0.019172	Half
122	25.602	0.512	0.080	0.022598	Max
123	-50.399	-1.004	0.069	0.022598	End

Max U ppm=2400.000		Max P ppm= 0.120		mm/yr= 10.0	
Time	U238 kg	U235 kg	Pu239 kg	eff enrch	
0	9314.300	126.800	44.200	0.018028	Start
0	9314.300	126.800	44.200	0.018028	Min
35	3974.575	73.415	10.072	0.020573	Half
61	22.779	0.663	3.268	0.147159	Max
62	-127.876	-3.590	3.126	0.147159	End

Max U ppm= 120.000		Max P ppm= 0.120		mm/yr= 10.0	
Time	U238 kg	U235 kg	Pu239 kg	eff enrch	
0	8905.000	94.400	61.800	0.017238	Start
138	7852.351	136.981	0.003	0.017146	Min
9	8836.031	112.658	42.346	0.017240	Max
139	7844.731	136.849	-0.005	0.017146	End

Max U ppm= 150.000		Max P ppm=		0.120 mm/yr= 10.0		
Time	U238 kg	U235 kg	Pu239 kg	eff	enrich	
0	8905.000	94.400	61.800	0.017238		Start
138	7589.226	132.667	0.003	0.017181		Min
29	8627.708	133.302	18.230	0.017260		Max
139	7579.702	132.501	-0.005	0.017181		End

Max U ppm= 200.000		Max P ppm=		0.120 mm/yr= 10.0		
Time	U238 kg	U235 kg	Pu239 kg	eff	enrich	
0	8905.000	94.400	61.800	0.017238		Start
0	8905.000	94.400	61.800	0.017238		Min
45	8331.818	137.519	9.240	0.017309		Max
139	7138.007	125.224	-0.005	0.017241		End

Max U ppm=1200.000		Max P ppm=		0.120 mm/yr= 10.0		
Time	U238 kg	U235 kg	Pu239 kg	eff	enrich	
0	8905.000	94.400	61.800	0.017238		Start
0	8905.000	94.400	61.800	0.017238		Min
65	3944.126	72.916	3.894	0.019103		Half
116	65.346	1.327	0.294	0.024212		Max
117	-10.631	-0.204	0.274	0.024212		End

Max U ppm=2400.000		Max P ppm=		0.120 mm/yr= 10.0		
Time	U238 kg	U235 kg	Pu239 kg	eff	enrich	
0	8905.000	94.400	61.800	0.017238		Start
0	8905.000	94.400	61.800	0.017238		Min
35	3556.048	63.548	14.140	0.021380		Half
58	60.517	1.691	5.284	0.103349		Max
59	-90.307	-2.311	5.060	0.103349		End

This program is used to check one case of the above output

Source program "c:\temp\maxrich.c"

The following program decrements the contents of the three principal isotopes just like richstat.c, but prints out the concentrations at each year, so that the max and min calculations of richstat.c can be verified.

```
/* maxrich.c Program to remove fissile material from SNF in a waste
package while decaying the Pu239 to U235. Program reads input
of 6 parameters per line/case (max ppm U, max ppm Pu, mm/yr infiltration,
initial kg U235, initial kg Pu239, initial kg U238) from the
input file "maxrich.in" until the file is exhausted. For each case
the components U238, U235, and Pu239 are decremented until one of them
is exhausted. */
```

```
#include <stdio.h>
```

1:36 pm

I-5

May 28, 1996

```
#include <stdlib.h>
```

```
main()
```

```
{int i; //time in 1000 year steps
```

```
float mu238, //mass of U238
```

```
mu235, //mass of U235
```

```
oldmu235, //temporary variable for consistency in updating
```

```
mp239, //mass of Pu239
```

```
maxu, //solubility of uranium, ppm
```

```
maxp, //solubility of plutonium, ppm
```

```
infl, //infiltration rate, mm/yr
```

```
pkgarea=6.46, //pkg cross-section area, sq meters
```

```
volflow, //volumetric flow through the package
```

```
pdr=1/24.4, //Pu decay rate per 1000 years
```

```
eenr; //effective enrichment (U235+Pu239)/(U238+U235+Pu239)
```

```
FILE *fin,*fout;
```

```
fin=fopen("maxrich.in","r");
```

```
fout=fopen("maxrich.out","w");
```

```
while(fscanf(fin,"%f %f %f %f %f %f",
```

```
&maxu,&maxp,&infl,&mu235,&mp239,&mu238)!=EOF)
```

```
{volflow=infl*pkgarea*.001; //vertical velocity times area
```

```
fprintf(fout,"\n\nMax U ppm=%8.3f Max P ppm=%6.3f mm/yr=%7.1f\n",
```

```
maxu,maxp,infl); //print header for this case
```

```
fprintf(fout,"Ini235=%f Ini239=%f\n",mu235,mp239);
```

```
fprintf(fout,"%12s%12s%12s%12s%12s\n","Time", "U238 kg", "U235 kg",
```

```
"Pu239 kg", "eff enrich"); //Column headings
```

```
i=0;
```

```
while((mu238>0)&&(mu235>0)&&(mp239>0)) //loop while all masses > 0
```

```
{eenr=(mu235+1.25*mp239)/(mu238+mu235+mp239); //effective enrichment
```

```
oldmu235=mu235; //Save for consistency in updating mu238
```

```
fprintf(fout,"%12d%12.3f%12.3f%12.3f%12.6f\n",
```

```
i,mu238,mu235,mp239,eenr); //output for this time
```

```
mu235=mu235-volflow*maxu*mu238/(mu235+mu238)+pdr*mp239*235/239;
```

```
//update U235
```

```
mp239-=pdr*mp239+volflow*maxp; //decrement Pu239
```

```
mu238-=volflow*maxu*mu238/(oldmu235+mu238); //decrement U238
```

```
i++;}}
```

Input file "c:\temp\maxrich.in"

The third case of the richstat.c set of 10 has been selected for verification

200 .12 10 126.8 44.2 9314.3

Output file "c:\temp\maxrich.out"

Max U ppm= 200.000 Max P ppm= 0.120 mm/yr= 10.0

Ini235=126.800003 Ini239=44.200001

Time	U238 kg	U235 kg	Pu239 kg	eff enrich
0	9314.300	126.800	44.200	0.018028
1	9301.554	128.408	42.381	0.018030

2	9288.810	129.940	40.636	0.018032
3	9276.067	131.399	38.963	0.018035
4	9263.328	132.789	37.358	0.018036
5	9250.591	134.111	35.820	0.018038
6	9237.855	135.370	34.344	0.018040
7	9225.122	136.568	32.928	0.018042
8	9212.391	137.706	31.571	0.018043
9	9199.661	138.788	30.270	0.018045
10	9186.934	139.816	29.021	0.018046
11	9174.207	140.792	27.824	0.018048
12	9161.482	141.718	26.676	0.018049
13	9148.759	142.596	25.575	0.018050
14	9136.037	143.428	24.519	0.018051
15	9123.316	144.216	23.506	0.018052
16	9110.598	144.963	22.535	0.018053
17	9097.880	145.668	21.604	0.018054
18	9085.163	146.335	20.711	0.018055
19	9072.448	146.965	19.854	0.018055
20	9059.734	147.559	19.033	0.018056
21	9047.021	148.119	18.245	0.018057
22	9034.310	148.646	17.490	0.018057
23	9021.599	149.142	16.765	0.018058
24	9008.889	149.607	16.070	0.018058
25	8996.180	150.044	15.404	0.018059
26	8983.472	150.453	14.765	0.018059
27	8970.765	150.835	14.152	0.018059
28	8958.059	151.192	13.564	0.018060
29	8945.354	151.524	13.000	0.018060
30	8932.648	151.832	12.460	0.018060
31	8919.944	152.119	11.941	0.018060
32	8907.241	152.383	11.444	0.018060
33	8894.538	152.627	10.968	0.018061
34	8881.836	152.851	10.510	0.018061
35	8869.135	153.056	10.072	0.018061
36	8856.434	153.243	9.651	0.018061
37	8843.733	153.412	9.248	0.018060
38	8831.034	153.564	8.861	0.018060
39	8818.335	153.700	8.490	0.018060
40	8805.637	153.821	8.135	0.018060
41	8792.938	153.927	7.793	0.018060
42	8780.241	154.019	7.466	0.018060
43	8767.544	154.097	7.153	0.018060
44	8754.847	154.162	6.852	0.018059
45	8742.150	154.215	6.563	0.018059
46	8729.454	154.255	6.286	0.018059
47	8716.759	154.284	6.021	0.018058
48	8704.063	154.302	5.766	0.018058
49	8691.368	154.310	5.522	0.018058
50	8678.674	154.307	5.288	0.018057



51	8665.979	154.294	5.064	0.018057
52	8653.285	154.272	4.849	0.018056
53	8640.592	154.241	4.642	0.018056
54	8627.898	154.202	4.444	0.018056
55	8615.205	154.154	4.254	0.018055
56	8602.512	154.098	4.072	0.018055
57	8589.819	154.035	3.897	0.018054
58	8577.127	153.964	3.730	0.018054
59	8564.435	153.887	3.569	0.018053
60	8551.742	153.803	3.415	0.018052
61	8539.051	153.712	3.268	0.018052
62	8526.359	153.615	3.126	0.018051
63	8513.668	153.513	2.990	0.018051
64	8500.977	153.404	2.860	0.018050
65	8488.285	153.290	2.735	0.018049
66	8475.595	153.172	2.615	0.018049
67	8462.904	153.048	2.500	0.018048
68	8450.214	152.919	2.390	0.018048
69	8437.523	152.785	2.284	0.018047
70	8424.833	152.648	2.183	0.018046
71	8412.143	152.506	2.086	0.018046
72	8399.453	152.360	1.992	0.018045
73	8386.764	152.210	1.903	0.018044
74	8374.074	152.056	1.817	0.018043
75	8361.385	151.899	1.735	0.018043
76	8348.695	151.738	1.656	0.018042
77	8336.006	151.575	1.580	0.018041
78	8323.316	151.407	1.508	0.018040
79	8310.627	151.237	1.438	0.018040
80	8297.938	151.064	1.372	0.018039
81	8285.248	150.889	1.308	0.018038
82	8272.560	150.710	1.246	0.018037
83	8259.871	150.529	1.188	0.018037
84	8247.183	150.346	1.131	0.018036
85	8234.494	150.160	1.077	0.018035
86	8221.806	149.972	1.025	0.018034
87	8209.117	149.782	0.975	0.018033
88	8196.429	149.590	0.928	0.018033
89	8183.740	149.396	0.882	0.018032
90	8171.052	149.200	0.838	0.018031
91	8158.363	149.002	0.796	0.018030
92	8145.675	148.802	0.756	0.018029
93	8132.987	148.601	0.717	0.018029
94	8120.299	148.398	0.680	0.018028
95	8107.611	148.193	0.644	0.018027
96	8094.923	147.987	0.610	0.018026
97	8082.235	147.780	0.577	0.018025
98	8069.547	147.571	0.546	0.018024
99	8056.859	147.361	0.516	0.018023

100	8044.171	147.150	0.487	0.018022
101	8031.483	146.937	0.459	0.018022
102	8018.795	146.724	0.432	0.018021
103	8006.107	146.509	0.407	0.018020
104	7993.419	146.293	0.383	0.018019
105	7980.731	146.077	0.359	0.018018
106	7968.043	145.859	0.337	0.018017
107	7955.355	145.640	0.315	0.018016
108	7942.667	145.421	0.294	0.018015
109	7929.980	145.200	0.275	0.018014
110	7917.292	144.979	0.256	0.018014
111	7904.605	144.757	0.237	0.018013
112	7891.917	144.534	0.220	0.018012
113	7879.230	144.311	0.203	0.018011
114	7866.542	144.086	0.187	0.018010
115	7853.855	143.861	0.172	0.018009
116	7841.167	143.636	0.157	0.018008
117	7828.480	143.410	0.143	0.018007
118	7815.792	143.183	0.129	0.018006
119	7803.105	142.956	0.116	0.018005
120	7790.417	142.728	0.104	0.018004
121	7777.730	142.500	0.092	0.018003
122	7765.042	142.271	0.080	0.018002
123	7752.355	142.042	0.069	0.018001
124	7739.667	141.812	0.058	0.018000
125	7726.980	141.582	0.048	0.017999
126	7714.292	141.352	0.039	0.017998
127	7701.605	141.121	0.029	0.017997
128	7688.917	140.889	0.020	0.017997
129	7676.230	140.658	0.012	0.017996
130	7663.542	140.426	0.003	0.017995

The following program is used to generate the data for approximation B of Section 7.3.

Source code "c:\temp\richsta.c"

This program demonstrates the effect of weighting the Pu concentration by a factor of 1.25 with respect to  $^{235}\text{U}$ . The differences are explained in Section 7.3.

```
/* richsta.c Program to remove fissile material from SNF in a waste
package while decaying the Pu239 to U235. Program reads input
of 6 parameters per line/case (max ppm U, max ppm Pu, mm/yr infiltration,
initial kg U235, initial kg Pu239, initial kg U238) from the
input file "richsta.in" until the file is exhausted. For each case
the components U238, U235, and Pu239 are decremented until one of them
is exhausted. This program also does the following:
(1) Determines the maximum and minimum
effective fissile percent and prints the concentrations and time at
```

which the maximum and minimum occur; (2) Prints a set of halfway statistics when the fissile content is half the initial value, if such a condition occurs before one of the nuclide species is exhausted. In addition to these special points, the program prints the starting and ending values of concentration and effective enrichment. This version of the program implements a factor of 1.25 multiplying the Pu239 concentration to account for the extra neutron efficiency which can occur under some circumstances.\*/\*

```
#include <stdio.h>
#include <stdlib.h>

void main()
{int year, //Counts time in intervals of 1000 years
  yearmax, yearmin, //Times (in 1000 years) of max and min eenr occur
  yearhalf, //Year at which the fissile content is half the starting value
  foundhalf, //Indicator of whether a half fissile has occurred by the time
              //one of the species is depleted, for this case.
  float mu238, //Current mass of U238 kg (decremented at each iteration)
  mu235, //Current mass of U235
  oldmu235, //Temporary value for consistency in updating
  mp239, //Current mass of Pu239
  maxu, maxp, //Solubilities of U and Pu, ppm
  infl, //Infiltration rate, mm/yr.
  pkgarea=6.46, //Horizontal cross section in sq meters
  volflow, //Vertical volumetric flow rate through a waste package, m3/yr.
  pdr=1/24.4, //Pu decay rate, per 1000 yrs
  fissile, //Plutonium plus U235
  mtotal, //Total of all three isotopes (fissile+U238)
  eenr, //Effective enrichment (fissile/mtotal)
  eenrmax, pumax, u238max, u235max, //maximum effective enrichment and
                                     //associated mass parameters
  eenrmin, pumin, u238min, u235min, //minimum effective enrichment and
                                     //associated mass parameters
  eenrhalf, puhalf, u238half, u235half, //parameters associated with the
                                     //50% fissile depletion point
  eenrstart, pustart, u238start, u235start; //Initial values
FILE *fin, *fout;
fin=fopen("richsta.in", "r");
fout=fopen("richsta.out", "w");
while(fscanf(fin, "%f %f %f %f %f",
             &maxu, &maxp, &infl, &mu235, &mp239, &mu238) != EOF) //read parameters and
                                                                    //initial values for this case
{volflow=infl*pkgarea*.001; //compute volumetric flow m3/yr
fprintf(fout, "\n\nMax U ppm=%8.3f  Max P ppm=%8.3f  mm/yr=%7.1f\n",
        maxu, maxp, infl); //print parameter value header for this case
fprintf(fout, "%6s%12s%12s%12s\n", "Time", "U238 kg", "U235 kg",
        "Pu239 kg", "eff enrch"); //print column headings for this case
```

```

year=0; //Initialize starting time for this case
foundhalf=0; //Start with no halfway point for this case
yearmax=yearmin=0; //Initialize max and min times to start
pustart=pumax=pumin=mp239; //Initialize mass values to starting values
u238start=u238max=u238min=mu238;
u235start=u235max=u235min=mu235;
fissile=mu235+1.25*mp239; //compute adjusted initial fissile
mtotal=fissile+mu238; //compute initial total mass
eenrstart=fissile/mtotal; //compute initial effective enrichment
eenrmax=eenrmin=eenrstart; //initialize max and min of eenr
while((mu235>0)&&(mp239>0)) //Loop until one of the fissile is depleted
{fissile=mu235+1.25*mp239; //Update fissile
mtotal=fissile-.25*mp239+mu238; //Update mtotal minus adjustment to
fissile
eenr=fissile/mtotal; //Update effective enrichment
oldmu235=mu235; //Compute temporary mass for update consistency
if(eenr>eenrmax) //Update maximum eenr point if appropriate
{eenrmax=eenr;
yearmax=year;
u238max=mu238;
u235max=mu235;
pumax=mp239;}
else if(eenr<eenrmin) //Update min eenr point if appropriate
{eenrmin=eenr;
yearmin=year;
u238min=mu238;
u235min=mu235;
pumin=mp239;}
if((foundhalf==0)&&(fissile<.5*(u235start+1.25*pustart)))
{foundhalf=1; //Test for halfway point and update as appropriate
yearhalf=year;
puhalf=mp239;
u235half=mu235;
u238half=mu238;
eenrhalf=eenr;}
//The next 3 lines are the basic updating equations for each iteration
mu235=mu235-volflow*maxu*mu235/(mu235+mu238)+pdr*mp239*235/239;
mp239-=pdr*mp239+volflow*maxp;
mu238-=volflow*maxu*mu238/(oldmu235+mu238);
year++;}
fprintf(fout, "%6d%12.3f%12.3f%12.3f%12.6f%12s\n",
0, u238start, u235start, pustart, eenrstart, "Start");
fprintf(fout, "%6d%12.3f%12.3f%12.3f%12.6f%12s\n",
yearmin, u238min, u235min, pumin, eenrmin, "Min");
if(foundhalf==1) fprintf(fout, "%6d%12.3f%12.3f%12.3f%12.6f%12s\n",
yearhalf, u238half, u235half, puhalf, eenrhalf, "Half");
fprintf(fout, "%6d%12.3f%12.3f%12.3f%12.6f%12s\n",
yearmax, u238max, u235max, pumax, eenrmax, "Max");
fprintf(fout, "%6d%12.3f%12.3f%12.3f%12.6f%12s\n",

```

```
year, mu238, mu235, mp239, eenr, "End");}}
```

## Input file "c:\temp\richsta.in"

The parameters of these cases are the same as those used for richstat.c, except that the maximum uranium solubility (maxu) values start much higher. This was done to identify a much higher minimum value for maxu at which the time history shows a maximum in fissile percent.

maxu	maxp	infl	mu235	mp239	mu238
800	.12	10	126.8	44.2	9314.3
1000	.12	10	126.8	44.2	9314.3
1200	.12	10	126.8	44.2	9314.3
1500	.12	10	126.8	44.2	9314.3
2000	.12	10	126.8	44.2	9314.3
2400	.12	10	126.8	44.2	9314.3
800	.12	10	94.4	61.8	8905
1000	.12	10	94.4	61.8	8905
1200	.12	10	94.4	61.8	8905
1500	.12	10	94.4	61.8	8905
2000	.12	10	94.4	61.8	8905
2400	.12	10	94.4	61.8	8905

## Output file "c:\temp\richsta.out"

Max U ppm= 800.000    Max P ppm= 0.120    mm/yr= 10.0

Time	U238 kg	U235 kg	Pu239 kg	eff enrch	
0	9314.300	126.800	44.200	0.019171	Start
130	2713.760	51.404	0.003	0.018591	Min
90	4742.614	89.235	0.838	0.018682	Half
0	9314.300	126.800	44.200	0.019193	Max
131	2663.041	50.444	-0.004	0.018591	End

Max U ppm=1000.000    Max P ppm= 0.120    mm/yr= 10.0

Time	U238 kg	U235 kg	Pu239 kg	eff enrch	
0	9314.300	126.800	44.200	0.019171	Start
130	1065.045	20.518	0.003	0.018905	Min
73	4678.135	88.195	1.903	0.018995	Half
0	9314.300	126.800	44.200	0.019193	Max
131	1001.666	19.297	-0.004	0.018905	End

Max U ppm=1200.000    Max P ppm= 0.120    mm/yr= 10.0

Time	U238 kg	U235 kg	Pu239 kg	eff enrch	
0	9314.300	126.800	44.200	0.019171	Start
14	8244.759	130.307	24.519	0.019162	Min
62	4588.339	86.436	3.126	0.019313	Half
122	25.602	0.512	0.080	0.023362	Max
123	-50.399	-1.004	0.069	0.023362	End

Max U ppm=1500.000		Max P ppm=		0.120 mm/yr=	10.0	
Time	U238 kg	U235 kg	Pu239 kg	eff enrch		
0	9314.300	126.800	44.200	0.019171		Start
0	9314.300	126.800	44.200	0.019171		Min
51	4453.747	83.545	5.064	0.019786		Half
97	82.223	1.730	0.577	0.029006		Max
98	-12.680	-0.244	0.546	0.029006		End

Max U ppm=2000.000		Max P ppm=		0.120 mm/yr=	10.0	
Time	U238 kg	U235 kg	Pu239 kg	eff enrch		
0	9314.300	126.800	44.200	0.019171		Start
0	9314.300	126.800	44.200	0.019171		Min
40	4229.713	78.544	8.135	0.020552		Half
73	49.360	1.174	1.903	0.067754		Max
74	-76.838	-1.751	1.817	0.067754		End

Max U ppm=2400.000		Max P ppm=		0.120 mm/yr=	10.0	
Time	U238 kg	U235 kg	Pu239 kg	eff enrch		
0	9314.300	126.800	44.200	0.019171		Start
0	9314.300	126.800	44.200	0.019171		Min
34	4126.819	75.787	10.510	0.021107		Half
61	22.779	0.663	3.268	0.177743		Max
62	-127.876	-3.590	3.126	0.177743		End

Max U ppm= 800.000		Max P ppm=		0.120 mm/yr=	10.0	
Time	U238 kg	U235 kg	Pu239 kg	eff enrch		
0	8905.000	94.400	61.800	0.018911		Start
138	1892.170	35.101	0.003	0.018215		Min
85	4581.582	83.583	1.579	0.018333		Half
0	8905.000	94.400	61.800	0.018943		Max
139	1841.432	34.160	-0.005	0.018215		End

Max U ppm=1000.000		Max P ppm=		0.120 mm/yr=	10.0	
Time	U238 kg	U235 kg	Pu239 kg	eff enrch		
0	8905.000	94.400	61.800	0.018911		Start
34	6738.783	110.220	14.753	0.018745		Min
70	4453.125	81.439	3.123	0.018808		Half
0	8905.000	94.400	61.800	0.018943		Max
139	78.214	1.499	-0.005	0.018833		End

Max U ppm=1200.000		Max P ppm=		0.120 mm/yr=	10.0	
Time	U238 kg	U235 kg	Pu239 kg	eff enrch		
0	8905.000	94.400	61.800	0.018911		Start
0	8905.000	94.400	61.800	0.018911		Min

BB0000000-01717-2200-00037 REV 00

Attachment I

60	4324.739	79.008	4.844	0.019295	Half
116	65.346	1.327	0.294	0.025310	Max
117	-10.631	-0.204	0.274	0.025310	End

Max U ppm=1500.000		Max P ppm=		0.120 mm/yr=	10.0	
Time	U238 kg	U235 kg	Pu239 kg	eff enrch		
0	8905.000	94.400	61.800	0.018911		Start
0	8905.000	94.400	61.800	0.018911		Min
50	4132.322	75.127	7.460	0.020037		Half
93	45.667	1.032	1.076	0.049754		Max
94	-49.092	-1.066	1.024	0.049754		End

Max U ppm=2000.000		Max P ppm=		0.120 mm/yr=	10.0	
Time	U238 kg	U235 kg	Pu239 kg	eff enrch		
0	8905.000	94.400	61.800	0.018911		Start
0	8905.000	94.400	61.800	0.018911		Min
39	3938.947	70.389	11.932	0.021213		Half
70	12.139	0.421	3.123	0.275775		Max
71	-112.729	-3.785	2.987	0.275775		End

Max U ppm=2400.000		Max P ppm=		0.120 mm/yr=	10.0	
Time	U238 kg	U235 kg	Pu239 kg	eff enrch		
0	8905.000	94.400	61.800	0.018911		Start
0	8905.000	94.400	61.800	0.018911		Min
34	3708.391	65.650	14.753	0.022195		Half
58	60.517	1.691	5.284	0.122921		Max
59	-90.307	-2.311	5.060	0.122921		End

1:36 pm

I-14

May 28, 1996

**Upper bound on the probability of formation of a reducing zone capable of collecting a critical mass,  $Pr\{\text{cluster}|\log\}$** **Background and Introduction**

The purpose of this analysis is to estimate an upper bound for the probability of achieving specified levels of uranium concentration in specified volumes of Yucca Mountain tuff below the water table by natural processes. This probability upper bound will be used to estimate the upper bound of the probability of achieving a critical mass of uranium as a result of transport and re-concentration of uranium from a commercial spent fuel repository.

Since, calculation of the dispersion and re-concentration of the uranium from SNF is a complex transport and chemical process, application of computer codes would be a lengthy process, and would not easily support straightforward estimation of worst case probabilities. An upper bound on probability might more readily be found from statistics of the known uranium deposits, using the *assumption that whatever processes precipitated uranium from groundwaters over geologic time would be the processes most likely to precipitate uranium from groundwaters having their charging source in a nuclear waste repository (if and when such a charging process were to take place)*. It may be argued that an SNF repository would be a much more concentrated source than is ever likely to have occurred in nature. However, the concentration of the repository source is likely to be quite dispersed by the time it reaches any reducing zones capable of concentrating a single critical mass orebody. This process of upper bound by analog is valid, even though the Colorado Plateau sandstone to be used as the statistical basis is quite different from the tuff below the repository, as long as it can be shown that the uranium deposits found in sandstone are richer (both higher concentration and larger orebodies) than those found in tuff.

**Methodology**

Investigations at Yucca Mountain have thus far revealed no evidence of a reducing zone, which would be required to concentrate a uranium bearing groundwater flow from the repository to the more than 1.6 metric tons of uranium, which is taken to be at 1.94% fissile enrichment, corresponding to the design basis PWR fuel) required to produce external criticality, as shown by Ref. 5.43. Therefore, a conservative upper bound for the probability of formation of a large uranium deposit is obtained from analysis of known deposits in the richest uranium area of the United States. The basis for this methodology is the *assumption that any reducing zone which might be found at Yucca Mountain could have no more uranium*



*precipitation capability than the concentration of uranium already found in this richest area of the United States. This is a generalization of assumption 4.3.7.*

The highest local uranium ore concentrations in the United States are found in the Uravan Mineral Belt in southwestern Colorado and southeastern Utah. The richest ores are found in carbonaceous logs along pre-historic river channels. These logs appear to come from the trunks of trees which fell into river channels, which were quickly buried and ultimately became sandstone. The concentrations of uranium required for criticality can be modeled by the juxtaposition of such logs onto a circle through the cross section of the critical mass sphere, to achieve the specified critical mass (upwards of 1 metric ton  $\text{UO}_2$ ). This model rests on the *assumption that the logs are uniformly, and independently, distributed throughout the mineralized orebody in which they are found.* This assumption is verified by statistical analysis of log locations in a single mining area, described later in this Attachment. The following paragraphs describe the general probability methodology for the analysis. The use of actual observations and statistical data construct very conservative distributions for the relevant log parameters will be described afterward.

The probability that a given log, equally likely to be found anywhere in the mineralized area A, has center falling within  $r$  and  $r+dr$  of the cross section circle (called the critical mass circle) center

$$p_1 = 2\pi r(dr)/A,$$

where it has been assumed that  $dr \ll r$ .

The probability that a log having its center falling within  $r$  and  $r+dr$  of critical mass circle center will have the proper orientation to overlap the critical mass circle (having radius  $r_c$ ) can be approximated by

$$p_2 = 2r_c/(\pi r),$$

which is simply the ratio of the arc subtended (with respect to the log center) by the diameter of the critical mass circle, divided by the arc of a semicircle.

The problem is further simplified by *assuming that the log will only be able to overlap the critical mass circle if its center is located so that the end of the log can overlap the critical mass circle center ( $r < l/2$ , where  $l$  is the length of the log).* This approximation means that a log will be counted as completely overlapping if it has more than 50% overlap, and otherwise it will be counted as non-overlapping. The

probability of overlap is then computed as the product of these two probabilities integrated over  $0 < r < l/2$ . Multiplying this product ( $p_1 p_2$ ) by the number of logs,  $n$ , in the area  $A$  gives the probability of one log overlapping the circle

$$p_l = 2r_c l p_l \quad (1)$$

where  $p_l = n/A$  is the density of logs in the overall orebody, and where the subscript  $l$  has been introduced for the log length to indicate that the log length will be treated as a random variable with value to be determined by a Monte Carlo sampling process, which will also determine the value of the dependent random variable  $p_l$ . It should be noted that Eqn. (1) could have been derived directly as the area of the rectangle defined by the length of the log and the diameter of the critical mass circle, multiplied by the density of logs per unit area.

The number of overlapping logs required for criticality is determined by adding successive logs until their contributed masses total the required critical mass ( $M$ ). Since overlapping the logs have random orientations, they will form a star shaped object, with the narrow branches suffering a large amount of neutron leakage and contributing little to the criticality. The first order estimate of contributing mass is, therefore, determined by that portion of the log length which actually overlaps the target circle

$$m_j = 2.62\pi r_l^2 (4/\pi) r_c u_j \quad (2)$$

where  $2.62 \text{ g/cm}^3$  is the density of tuff (which is conservative because the logs found in the Uravan Mineral belt are mostly coal, which has half this density);  $r_l$  is the radius of the log; the factor  $(4/\pi)r_c$  is the average length of segment falling within a circle of radius  $r_c$  for a longer line passing entirely through the circle; and  $u_j$  is a random variable representing the weight percent of uranium in the log, with the subscript  $j$  to indicate that its Monte Carlo selection process will be distinct from the Monte Carlo selection of the log length. The mass contribution used in the calculations will be adjusted upward (by a factor of 2) according to the methodology described later in this attachment.

#### Theoretical log spacing statistics

To test the assumption of random independent spatial distribution for the mineralized logs, the average nearest neighbor and next nearest neighbor distances were calculated from the analysis of the orebody map in Fischer (Ref 5.28, plate 57). These were compared with the theoretical values for a random spatial distribution having the same log density ( $p_l$ ).

The asymptotic approximation (for large  $n$ ) to the theoretical nearest neighbor distances is computed as follows:

Consider  $n$  points uniformly, and independently, distributed on the unit square. The density of points is  $p=n$ . For large  $n$ , the probability density function (pdf) for the nearest neighbor distance is computed by considering a probability that a single point falls within a circular ring ( $r$  to  $r+dr$ ) centered around a given point while all the other points fall outside the ring:

$$(pdf_1)dr = (n-1)(2\pi r)dr(1-\pi r^2)^{n-2} \quad (3)$$

which is the product of the number of ways of selecting the point to fall within the ring ( $n-1$ ) multiplied by the probability of a single point falling within the ring ( $2\pi r dr$ ), multiplied by the probability that the remaining  $n-2$  points all fall outside the ring  $(1-\pi r^2)^{n-2}$ . The third factor is only correct as long as the circle is not close to the boundary of the unit square, or for  $r \ll 1$ . For  $n \gg 1$  the factor will be very small unless  $r \ll 1$ , so the approximation is valid. With this pdf, the mean value of the nearest neighbor distance is

$$\langle r_{nn} \rangle = \int_0^{1/\sqrt{\pi}} r (pdf_1) dr$$

where the upper limit of integration is chosen somewhat arbitrarily so that the third factor of pdf<sub>1</sub> does not go below 0, and which doesn't affect the result in the asymptotic limit. This integral can be evaluated analytically as it stands, but it is illustrative of the asymptotic approximation if the variable is changed to  $r = z/(\pi n)^{1/2}$ , and the following substitution (valid for  $n \gg 1$ ) is used

$$(1-z^2/n)^n = \exp(-z^2).$$

The integral becomes

$$\langle r_{nn} \rangle = 2 \int_0^{\sqrt{n}} z^2 \exp(-z^2) dz / \sqrt{\pi n}$$

where the  $n \gg 1, z^2$  has also been relied on for the simplification

$$((n-1)/n)(1-z^2/n)^{-2} \approx 1.$$

The approximation  $n \gg 1$  has the additional consequence that the integrand becomes very small as  $z$  approaches the upper limit, so the upper limit can be

approximated by  $\infty$ , and the integral can be easily evaluated to give

$$\langle r_{nn} \rangle = 1/(2n^{.5}) = 1/(2\rho_i^{.5}) \quad (4)$$

where the last form (with  $\rho_i$ ) is a generalization to an arbitrary area A.

For comparison between calculated and measured values it is necessary to also compute the standard deviation of the mean, which is defined as the standard deviation of the distribution divided by the square root of the number of points in the sample from which the mean is computed (which is just the number of logs in the sample). The standard deviation of the distribution is

$$\sigma_{nn} = (\langle r_{nn}^2 \rangle - \langle r_{nn} \rangle^2)^{.5}$$

where the mean square nearest neighbor distance is simply

$$\langle r_{nn}^2 \rangle = \int_0^\infty \frac{1}{\sqrt{\pi}} r^2 (pdf_1) dr$$

which can be transformed with the same substitution  $r = z/(\pi n)^{.5}$  as was used above, and the same asymptotic approximation to give

$$\langle r_{nn}^2 \rangle = 2 \int_0^\infty z^3 \exp(-z^2) dz / (\pi n)$$

This integral can be evaluated to give

$$\langle r_{nn}^2 \rangle = 1/(\pi n) = 1/(\pi \rho_i),$$

so that the standard deviation of the distribution is

$$\sigma_{nn} = (1/\rho_i^{.5})(1/\pi - 1/4)^{.5} = 0.52 \langle r_{nn} \rangle$$

The next nearest neighbor pdf is constructed in a manner similar to the nearest neighbor pdf, with the added complexity that the first point selected must fall inside the inner circle of the  $rdr$  ring. The probability is the product of the number of ways to select the first point ( $n-1$ ), multiplied by the number of ways to select the second point ( $n-2$ ), multiplied by the probability that the first point will fall within the inner circle of the ring ( $\pi r^2$ ), multiplied by the probability that the second

point will fall within the ring ( $2\pi r dr$ ), multiplied by the probability that the remaining  $n-3$  points will all fall outside the ring  $(1-\pi r^2)^{n-3}$ .

$$(pdf_2)dr = (n-1)(n-2)(\pi r^2)(2\pi r dr)(1-\pi r^2)^{n-3} \quad (5)$$

Using the same asymptotic approximation and variable substitution as for nearest neighbors, the mean next nearest neighbor distance becomes

$$\langle r_{nnn} \rangle = 2 \int_0^\infty \sqrt{\pi} z^4 \exp(-z^2) dz / \sqrt{\pi} \quad (6)$$

which can be evaluated to give

$$\langle r_{nnn} \rangle = 3n^{-5/4} \quad (7)$$

The standard deviation of the distribution of next-nearest neighbor distances can be calculated by the same steps as was done for the nearest neighbor distance, above. This leads to the integral approximating the mean square next-nearest neighbor distance

$$\langle r_{nnn}^2 \rangle = 2 \int_0^\infty z^5 \exp(-z^2) dz / (\pi n)$$

which can be evaluated and substituted into the equation for the standard deviation to give

$$\sigma_{nnn} = (1/\rho_1^{5/4})(2/\pi - 9/16)^{1/4} = 0.36 \langle r_{nnn} \rangle$$

The validity of these analytic approximations for nearest neighbor and next nearest neighbor distances is verified by the following program using the Monte Carlo process to generate randomly located points on the unit square, with the average nearest neighbor and next nearest neighbor distances computed for each iteration, together with the standard deviations for each. Agreement between the above asymptotic approximations and the Monte Carlo simulations is demonstrated by dividing the simulated output by the corresponding asymptotic approximation and printing the result.

```
/* 2dmin.c Monte Carlo calculation of mean nearest neighbor and next
nearest neighbor distances, and their standard deviations,
for points randomly distributed on a unit square
using a 2-d uniform distribution. The outputs are normalized by the
analytic asymptotic approximations of the nearest neighbor and next
```

nearest neighbor means and standard deviations, so that they should print out approximately 1 for each iteration. The iterations are characterized by increasing number of points. The program also verifies that the bias (amount by which the outputs differ from 1) decreases with increasing number of points. The bias for the first 25 cases (100 to 124 points) and the last 25 cases (175 to 199 points) are printed at the end of the output, and the latter is seen to be smaller than the former for each of the 4 parameters calculated. \*/

```
#include <stdlib.h>
#include <stdio.h>
#include <math.h>
#include <time.h>
#define M 200 //Maximum number of points

void main()
{int i,j,k; //Counting variables
float sum, //Variable to accumulate nearest neighbor distance
  nnsum, //To accumulate next nearest neighbor distance
  sumsq, //For accumulating nearest neighbor distances squared
  nnsumsq, //For accumulating nn neighbor distances squared
  sig, //Std deviation of nearest neighbor distance distribution
  signn, //Std deviation of next nearest neighbor distance distribution
  x[M],y[M], //Array of coordinates for the points
  z, //Temporary variable for distance between 2 points
  mind, //Current nearest neighbor distance to a given point
  nnmind, //Current next nearest neighbor distance
  rnn, //To be used for the analytic approx to the nn distance
  rnnn, //To be used for the analytic approx to the nnn distance
  asig, //For analytic approx to std deviation of nn distance distribution
  asignn, //For analytic approx to std dev of nnn distance distribution
  bias1[4]={0}, //temporary variables for accumulating the first 25 bias
  bias2[4]={0}; //temporary variables for accumulating the last 25 biases
FILE *fout;
fout=fopen("2dmin.out","w");
srand((unsigned)time(NULL));
fprintf(fout,"%8s%15s%15s%15s%15s\n", //Print headers for output file columns
  "Num pts","Nrmlzd nn dist","Nrmlzd nnn dist",
  "Nrmlzd nn sig","Nrmlzd nnn sig");
for(k=100;k<M;k++) //k simulates the number of points (up to M)
{sum=0; //Initialize summing variables for this iteration
  nnsum=0;
  sumsq=0;
  nnsumsq=0;
  for(i=0;i<k;i++) //Loop to generate k points at random locations
  {x[i]=(float)rand()/RAND_MAX; //on the unit square
  y[i]=(float)rand()/RAND_MAX;}
  for(i=0;i<k;i++) //Outer loop to find nearest neighbor to each point
  {mind=1.41; //Initialize minimum distances to largest possible
```

```

nnmind=1.41;
for(j=0;j<k;j++)//Inner loop to find nearest neighbor for point i
  if(i!=j)
    {z=sqrt((x[i]-x[j])*(x[i]-x[j])+(y[i]-y[j])*(y[i]-y[j]));
    if(mind>z) //If this distance is less than the current minimum
      {nnmind=mind; //Replace the current nn with the current nearest
      mind=z;} //Replace the current nearest with this distance (z)
    else if(nnmind>z) nnmind=z;}//If it's only less than the current
    //next nearest, replace the current next nearest with z.
nnsum+=nnmind;//Accumulate nn neighbor distance for all (k) points
nnsumsq+=nnmind*nnmind;//Accumulate sum of squares for std deviation
sumsq+=mind*mind;
sum+=mind;} //Accumulate nearest neighbor distance for all (k) points
rnn=.5/sqrt(k);//Asymptotic approx for mean nearest neighbor distance
rnnn=.75/sqrt(k);//Asymptotic approx for mean next nearest neighbor distance
asig=.5227*rnn; //Asymptotic approx for std deviation of nn distance
asig=.363*rnnn;//Asymptotic approx for std deviation of nnn distance
sig=sqrt(sumsq/k-sum*sum/pow(k,2));//Monte Carlo for std dev of nn distance
signn=sqrt(nnsumsq/k-nnsum*nnsum/pow(k,2));//MC for std dev of nnn distance
if(k<125) //Accumulate first 25 biases
  {bias1[0]+=sum/k/rnn-1;
  bias1[1]+=nnsum/k/rnnn-1;
  bias1[2]+=sig/asig-1;
  bias1[3]+=signn/asig-1;}
if(k>174) //Accumulate last 25 biases
  {bias2[0]+=sum/k/rnn-1;
  bias2[1]+=nnsum/k/rnnn-1;
  bias2[2]+=sig/asig-1;
  bias2[3]+=signn/asig-1;}
fprintf(fout,"%8d%15.5f%15.5f%15.5f%15.5f\n",
  k,sum/k/rnn,nnsum/k/rnnn,sig/asig,signn/asig);
printf("%d\n",k);}
for(i=0;i<4;i++)
  {bias1[i]/=25;
  bias2[i]/=25;}
fprintf(fout,"%8s%15.5f%15.5f%15.5f%15.5f\n","bias1",
  bias1[0],bias1[1],bias1[2],bias1[3]);
fprintf(fout,"%8s%15.5f%15.5f%15.5f%15.5f\n","bias2",
  bias2[0],bias2[1],bias2[2],bias2[3]);}

```

The output of this program is given in the following table, where the validity of the asymptotic approximation is demonstrated by the fact that the normalized numbers are all close to 1. The number of points for the Monte Carlo simulation has been taken from 100 to 199, even though the number of logs in the actual sample analysed is only 84, to demonstrate the decreasing bias (average deviation from 1) with increasing number of points. This demonstration is given by the last two lines of the output, which give the average bias for the first 25 cases (bias1) and the last 25 cases (bias2), and show a decrease between the former and the latter.

Num pts	Nrmlzd nn dist	Nrmlzd nnn dist	Nrmlzd nn sig	Nrmlzd nnn sig
100	1.08869	1.06213	0.94382	1.04738
101	1.07517	1.06526	1.02585	1.21354
102	1.06618	1.07300	1.20536	1.27991
103	0.98163	1.00157	1.09719	1.25437
104	1.04623	1.03570	1.07439	0.92141
105	0.95482	1.07586	1.06669	1.25606
106	1.02116	1.09554	1.12290	1.21179
107	1.03820	1.11080	1.17016	1.29951
108	1.05745	1.06537	1.15947	1.13815
109	1.12533	1.06494	1.20642	1.17941
110	1.05919	0.99697	1.03621	1.10726
111	0.91473	1.02404	1.09922	1.08689
112	1.09289	1.03391	1.16388	1.19414
113	1.01085	1.04372	1.21334	1.36906
114	1.08110	1.12346	1.25962	1.31923
115	1.07898	1.08189	1.27243	1.42170
116	1.12196	1.11435	1.11003	1.09462
117	1.01804	1.02566	0.97330	1.12571
118	1.00286	0.99870	1.11496	1.16189
119	1.05631	1.09375	1.09565	1.15869
120	1.05801	1.05209	1.04992	1.19064
121	0.93960	0.95084	0.97762	0.99485
122	1.05230	1.04469	1.11311	1.16220
123	1.08034	1.10855	1.18570	1.13278
124	1.08990	1.06436	1.01648	1.15614
125	1.02911	1.06575	1.16673	1.25975
126	1.01526	0.96528	1.02576	1.24053
127	1.13833	1.12918	1.18941	1.09135
128	1.10595	1.06461	1.10899	1.06250
129	1.08209	1.09550	1.06864	1.21437
130	1.02261	0.99174	1.08442	1.16653
131	1.07858	1.06729	1.18691	1.16727
132	1.08548	1.06213	1.02608	1.13075
133	0.98480	1.03945	1.10653	1.05439
134	0.99262	0.99171	1.21617	1.30328
135	1.09709	1.04444	1.16841	1.18198
136	1.06761	1.03848	0.98987	1.07978
137	1.10694	1.05828	1.07380	1.01858
138	0.99142	1.06752	0.97196	1.03923
139	0.99889	1.06362	0.99493	0.95036
140	1.01371	1.04257	0.99821	1.11546
141	0.98841	1.01086	1.05474	1.20221
142	1.02611	1.06939	1.07225	1.13400
143	1.05628	1.10111	1.09150	1.00229
144	1.06857	1.08963	1.19356	1.14469
145	0.99109	0.98911	1.08412	1.14527
146	0.96963	1.07730	0.99305	1.04697



147	1.08454	1.04046	1.06015	1.35516
148	1.03587	1.04841	1.07489	1.11144
149	1.05260	1.05092	1.08009	1.18303
150	0.97474	1.04817	1.03704	1.10162
151	0.97895	1.00491	1.02167	1.13178
152	1.07995	1.05697	1.10202	1.18644
153	1.04974	1.04534	0.95911	1.09905
154	1.11322	1.14338	1.02199	1.11866
155	1.04292	1.02256	1.02349	1.05241
156	1.14198	1.06769	0.99041	0.99503
157	1.11775	1.02058	1.13732	1.10083
158	1.03878	1.05814	0.99264	1.10785
159	1.08579	1.03583	1.32191	1.43464
160	1.09231	1.07682	0.96302	1.09794
161	1.00507	0.99988	1.04924	1.13461
162	0.99037	0.99882	1.14714	1.20439
163	1.02227	1.00426	1.23976	1.36551
164	1.07264	1.05260	1.08031	1.08034
165	1.04671	1.11109	1.09812	1.19430
166	1.05903	1.10265	1.13877	1.32242
167	1.07015	1.09099	1.12726	1.27863
168	1.02479	1.00864	1.20435	1.14919
169	1.03707	1.02834	1.09087	1.16718
170	1.08406	1.04427	1.07228	1.14018
171	0.94203	0.99859	1.11462	1.20434
172	1.10485	1.02532	1.05692	1.13679
173	0.99310	1.01561	1.10075	1.22871
174	1.02361	1.03142	1.00085	1.04277
175	1.00637	1.00225	1.05136	1.18861
176	1.01105	1.07423	1.12408	1.10481
177	1.10709	1.12062	1.22376	1.26774
178	1.04209	1.01704	1.15187	1.09968
179	1.08301	1.09728	1.18389	1.17510
180	0.98030	1.01460	1.01564	1.10702
181	0.96921	1.05306	1.05570	1.12615
182	1.07426	1.11400	1.00681	1.08062
183	1.07206	1.03682	1.25089	1.23719
184	0.97127	1.06118	1.03078	1.04252
185	0.99410	1.01518	1.09662	1.12341
186	0.99603	1.01099	1.11920	1.06958
187	0.98526	1.05919	1.02933	1.03281
188	1.03720	1.02158	1.09809	1.07672
189	1.02187	1.03651	0.99079	1.04472
190	1.00253	0.99323	1.04509	1.13582
191	0.95075	0.98327	0.94353	1.04432
192	0.96239	0.99616	1.09950	1.05987
193	1.05624	1.04157	1.03902	1.01607
194	1.02709	1.01664	1.02736	1.06514
195	1.01574	1.02020	1.08086	1.08920

196	1.09287	1.07952	1.17181	1.15705
197	1.08014	1.08818	1.20414	1.20104
198	1.07598	1.05854	1.16793	1.16964
199	0.96734	0.98951	0.97537	1.10731
bias1	0.04448	0.05629	0.11015	0.17909
bias2	0.02329	0.04005	0.08734	0.11289

Attachment III describes the analysis of the map in Fischer (Ref 5.28, plate 57) and gives  $\rho_l = 84/87100 = .000964$  logs/sq meter. This value of log density was used in the theoretical formulas given above for nearest neighbor and next nearest neighbor distance, and the results were compared to the values estimated from analysis of the Fischer map. The comparison are summarized by the following table, which also gives the standard deviation of the means  $(\sigma_{nn}, \sigma_{nnn})/n^{.5}$  for measuring the significance of the differences.

Parameter	Calc mean	Std dvtn of mean	Mean from map data
Nearest neighbor distance	16.1	0.92	15.0
Next-nearest neighbor distance	24.2	0.96	26.7

For nearest neighbor distances the theoretical and actual values differ by only 1.2 standard deviations of the mean. The comparison for next-nearest neighbor distance shows a difference of 2.6 standard deviations, which could be interpreted as a small deviation from randomness (mutual independence of log location). Since, however, the deviation is in the direction of non-clustering, the assumption of randomness is conservative for purposes of this analysis. This analysis will, therefore, use the assumption that the spatial distribution of logs is completely random, and there is no special clustering behavior.

#### Distribution of relevant log parameters

In this model, three log parameters are generated from specific distributions: log length, potential concentration of uranium, and log radius. For the distribution of log lengths, the analysis of Attachment III shows a negative exponential distribution with a floor of 3.0 meters and a decay length of 4.6 meters.

For potential concentration of uranium the following three observational data sets are used:

- Breger (Ref 5.8, table I, pg 102-105) gives characteristics of 64 samples of

logs mostly in the Uravan area, but also many from Wyoming, with an average concentration of 1.88 wt%, with the largest concentration in the set being 16.5 wt% (case 53 of the table). It should be noted that these weight fractions are with respect to the immediately surrounding rock, which was generally coal, which has a range of density, but 1.3 g/cm<sup>3</sup> (or metric tons/m<sup>3</sup>) is typical. Since this density is only half that of tuff, these wt% concentrations could be conservatively reduced by a factor of 2.

- Hess (Ref. 5.29, pg 467) has related a description provided to him relating to two logs having diameters 4 ft and 3 ft with lengths of 100 ft and 75 ft, respectively, which provided a total of 105 tons of ore containing 13650 lbs of U<sub>3</sub>O<sub>8</sub>. Converting these parameters into metric gives a total volume of 50.6 m<sup>3</sup>, an ore density of 1.88 metric tons/m<sup>3</sup>, a U<sub>3</sub>O<sub>8</sub> mass density of .122 metric tons per m<sup>3</sup>, and a wt% of 6.5%.
- Chenoweth (Ref 5.15, pg 166) relates logs as large as 15 meters long and 1 meter diameter (11.8 m<sup>3</sup>). He also relates an ore shipment of 9 tons which averaged 21.5wt% U<sub>3</sub>O<sub>8</sub> (Ref 5.15, pg 168), but does not give the ore material or state its density or volume. The 9 tons represents a volume only 58% of the maximum size log, even at the low coal density of 1.3 metric tons/m<sup>3</sup>. Therefore, either the shipment was less than a full log, or the log yielding the ore was less than 60% of the volume of the largest log, or there must have been some preliminary concentration of the ore by mechanical means (e.g. screening for the larger inclusions or nuggets of uraninite).

The last two of these data sets are also used to derive the conservative estimate of log radius distribution.

Based on the above 3 data sets, a uniform distribution between 1% and 21.5% is used for potential uranium concentration

$$f_c(x) = 1/(x_2 - x_1) \quad \text{for } x_1 < x < x_2$$

where x is expressed as a fraction (instead of a percent) to correspond to the actual mathematics of calculation used in the program listing below, and the constant values are  $x_1 = 0.01$ ,  $x_2 = 0.215$ . This distribution gives an average ore grade (U<sub>3</sub>O<sub>8</sub> concentration) of 11.25%.

This distribution is conservative with respect to the three data sets for the following reasons:

- The only data set based on actual laboratory analysis of rock samples (Breger 5.8) shows an average concentration much smaller than the average of this distribution. Even there maximum uranium concentration (16.5%) found in Ref 5.8, pg 105, also becomes less than the average of the distribution (11.25%)

when adjusted for the fact that the density of the host rock (coal) is less than half that of tuff.

- The data of Ref 5.29, pg 467 imply a maximum uranium concentration of 6.5%, again less than half the average of the uniform distribution proposed above.
- The maximum  $U_3O_8$  concentration in Ref 5.15, pg 168 (21.5%) is ambiguous, but it is used for the upper limit of the conservative model of potential uranium concentration.
- The limited number of higher concentrations outside the United States occur in in rock completely different from the tuff at Yucca Mountain. For example, the maximum of 60% reported for Oklo (Ref. 5.34, pg 20), occurs only in black shale or sandstone, neither of which is present at Yucca Mountain.

Furthermore, it should be noted that the uranium concentration will be expressed in terms of  $UO_2$ , which is 88% uranium by weight, while the mining data from which the the density distribution is derived is expressed in terms of  $U_3O_8$ , which is only 85% uranium by weight. Therefore, the use of this distribution in  $k_{eff}$  calculations has a small extra degree of conservatism with respect to the data from which it was derived.

For the distribution of log radii, the smallest of 4 diameters cited by Hess (Ref 5.29, pg 467), 16 inches (or radius of 20 cm) is taken as the lower limit of a triangular distribution. The upper limit of the radius distribution is taken to be 80 cm, well above the maximum diameter, 4 feet (61 cm radius) given by Hess. This distribution is a conservative model because the Hess article is primarily interested in reporting the largest ore concentrations, which would correspond to the largest logs. This conservative designation for the model is also consistent with the Chenoweth (Ref. 5.15, pg 166) statement cited above that the largest log diameter is 1 meter. The pdf for the resulting triangular distribution is

$$f_r(r) = 2(rl_2 - r)/(rl_2 - rl_1)^2 \quad \text{for } rl_1 < r < rl_2$$

where  $rl_1 = 0.20$  meter,  $rl_2 = 0.80$  meter.

#### Adjustment for non-overlapping log fraction

The preliminary analysis of the mass formed by overlapping logs leading to Eqn (2), above, was based on the assumption that only the fraction of the total log length defined by the segment cut by the critical circle was contributing to the critical mass. To the extent that the log juxtaposition might be considered as an actual physical process, and not simply a surrogate for more general (and more nearly

spherical) concentrations or carbonaceous material), this cut segment assumption is non-conservative because the neutronics contribution of the portion of the logs outside the circle is neglected. It is, therefore, necessary to construct an adjustment factor to include some neutronic effect from the portions of the log which extend beyond the critical sphere. The methodology is as follows:

- Define an outer shell which has twice the radius of the critical sphere, and assume that all logs are shortened to fit in this circle. *It is assumed that this extra layer will provide a conservative representation of the effect of the log segment outside of the inner critical sphere.*
- Model the log mass falling in the outer shell by a homogeneous distribution in such a way that the average density throughout the sphere plus shell system is one half the density for the center sphere. Since one eighth of the volume is in the inner sphere and 7 eighths is in the outer shell, the density of the outer shell is determined from the equation  $\rho_c/2 = \rho_c/8 + 7\rho_s/8$ , which can be solved for  $\rho_s$  to give  $\rho_s = 3\rho_c/7$ . This is a more conservative approach (larger density in the outer shell) than to assume that all the logs which intersect the circle go through the center so that the log mass in the outer shell would be equal to the log mass in the inner shell, which would give  $\rho_s = \rho_c/7$  for spherical spreading to the outer shell or  $\rho_s = \rho_c/3$  for cylindrical spreading (which spreads as a disk, in keeping with the general two dimensional layout and log orientation in the deposit described by Fisher (Ref. 5.28)).
- Compute the critical mass/radius for the sphere-shell combination having  $\rho_s = 3\rho_c/7$ , where  $\rho_c$  is the fissile density which gave the smallest critical mass in Ref. 5.43, and using the corresponding water and tuff concentrations. With those parameters, the adjusted critical mass is found to be 0.520 metric tons, and the critical radius 39.4 cm (Ref. 5.43).
- Determine a correction factor for critical mass to be the ratio of adjusted critical mass to the original critical mass ( $.52/1.6 = 0.325$ ) and the corresponding correction factor for radius ( $39.4/57.4 = 0.686$ ).
- Use the adjusted critical mass as the target to determine the number of logs required to accumulate. Use the adjusted radius (inner sphere radius) to define the length of *log segment to be used as the mass contribution of a single log*  $(4/\pi)r_c$ .
- Use the uncorrected sphere radius to determine the probability of overlap between log and critical circle according to Eqn. (1). This is justified because the corrected sphere was related to a reduced critical mass, while the overlap probability should still relate to the original geometry. Furthermore, this assignment is conservative in comparison with using the corrected sphere radius.

In the above described adjustment, the reduction in the target critical mass is a conservative adjustment, while the reduction in the critical radius is non-

conservative (reducing the contribution of the log to the critical mass). The net effect is conservative because the correction for mass is over a factor of 3 in the conservative direction while the correction for radius (or contribution) is less than a factor of 2 in the non-conservative direction.

The methodology can now be summarized by an algorithm stated as follows: (1) Determine a critical mass - critical radius pair from the set generated in Ref. 5.43, and apply the adjustment factors 0.325 and 0.686, respectively, as a measure of conservatism to account for the neutron contribution of the portions of the logs falling outside the critical sphere; (2) Select the three random parameters for a sample log from the appropriate distributions as described above (log length, log radius, uranium wt%); (3) Calculate the contributed mass for this log from Eq (2), above and accumulate the sum of the masses of overlapping logs thus far; (4) Multiply the accumulated probability by the value for this log as computed from Eq (1) using the uncorrected radius; (5) If the accumulated mass is greater than the required critical mass, end the calculation and report the remaining probability, otherwise repeat steps (2) through (5) for the next log. This algorithm is repeated, starting with step 1, for each critical mass - critical radius pair in the set generated in Ref. 5.43.

#### Calculation

This methodology is implemented by the following program

Source Code "c:\temp\prden.c" 5/20/1996

The input file which includes the set of critical masses for the bare sphere cases evaluated in Ref. 5.43, is

```
/* prden.c Program to compute the probability of log juxtaposition
sufficient to form a critical mass. Three log parameters are
generated by Monte Carlo sampling: the log length which determines
the probability of overlap, the log radius, which effects the
mass contributed by the log, and the potential uranium weight percent
in the log, which also effects the increment of critical mass which
the log provides. The program adds logs until a critical mass
would be reached. For each log added, the probability is multiplied
by a factor reflecting the probability of overlap for this size log.
The implementation algorithm is conservative, because the overlap
factor is only multiplied if the accumulated mass is less than the
critical mass. The additional log required to go beyond the critical
mass is not used so there is always some shortfall in the accumulation
of the critical mass. The estimated
value for the probability is computed by averaging over a number of
Monte Carlo iterations, specified by the parameter "num". Both
```

arithmetic and geometric mean are computed. The input file consists of one line containing the labels for the two input parameters (critical mass in metric tons, and critical radius in meters) followed by one line for each case, with each line containing a pair of input values for these two parameters. In this manner an arbitrary number of cases can be evaluated in one run.

It should be noted that this is not a complete calculation of the probability of such a mass actually occurring as the result of uranium enriched groundwater flow from a nuclear waste repository. That would require consideration of plume dispersion and probability of occurrence of a mineralized zone which could contain the logs in the first place. \*/

```
#include <stdlib.h>
#include <stdio.h>
#include <math.h>
#include <time.h>

void main()
{long int i,j=0,k,    //Counting variables
  num=1000; //Number of Monte Carlo iterations
int   firsttime=1, //Indicator variable for first case diagnostics
      count=0,    //Count number of cases
      firstlog;   //Indicator for first log to avoid probability mult
double p,         //Variable to accumulate the probability of overlap for a
          //single iteration
      psum,psumsq,logpsum,logpsumsq; //Variables for
          //accumulating statistics for all the iterations
float x, //Temporary variable for uranium weight percent
      y, //Temporary variable for log length
      sum, //Accumulation of overlapped uranium masses
      cmass=1, //Critical mass (this value overwritten by input file)
      x1=0.01, x2=0.213, //Limits of uniform distribution for uranium wt %
      rlmin=.20,rlmax=.80, //Min and max log radius
      rl, //Temporary variable for log radius generated randomly
      len0=10/3.28, //Minimum log length
      lend=1/.0656/3.28, //Decay length for negative exponential
          //log length distribution
      rc=3, //Radius of critical mass circle (overridden by input file)
      rho1=.000964, //Density of logs per square meter
      rhot=2.62, //Density of host rock (tuff in saturated zone)
      cfacr=.394/.574, //Correction factor for critical circle radius
      cfacm=.52/1.6; //Correction factor for critical mass
char dummy1[80],dummy2[80]; //Temporary variables
          //for reading the labels of the input parameters
FILE *fout,*fin,*ferr;
fout=fopen("prden.out","w"); //Output file
ferr=fopen("junk.out","w"); //Used for diagnostics and debugging
```

```

fin=fopen("prden.in","r");//Input parameters
fscanf(fin,"%s %s",dummy1,dummy2);//parameter names
fprintf(fout,"%8s %8s", dummy1,dummy2);//column heading prmtr names
fprintf(fout,"%11s%11s\n","Arith mean","Geom mean");
srand((unsigned)time(NULL));//random number seed selected from time count
while(fscanf(fin,"%f %f",&cmass,&rc)!=EOF) //Input parameters
{
    cmass*=cfacm; //Adjustment of target critical mass
    rc*=cfacr; //Adjustment of critical circle for probability calculation
    fprintf(fout,"%8.3f %8.3f",cmass,rc);//Print the input values this case
    psum=0;
    psumsq=0;
    logpsum=0;
    logpsumsq=0;
    for(i=0;i<num;i++)//Loop for each Monte Carlo iteration
    {
        p=1;//Initialize probability for this iteration
        sum=0;//Initialize sum of log contributions for this iteration.
        k=0;//Count number of logs required in this iteration
        firstlog=1; //Set to avoid multiplication for first log
        while(sum<cmass) //Loop to build the mass for a single iteration
        {
            x=x1+(x2-x1)*(float)rand()/RAND_MAX; //Generate uranium wt%
            rl=rlmax-(rlmax-rlmin)*sqrt(1-(float)rand()/RAND_MAX);//Generate radius
            y=(float)rand()/RAND_MAX;//Generate random variable for log length
            if(y==1) y=.9999; //Avoid singularity in log function next line
            y=len0+lend*log(1/(1-y)); //Compute log length from this random var
            k++;//Increment log count
            sum+=3.14159*rl*rl*4/3.14159*rc*x*rhot; //Accumulate mass for this
                //iteration using average segment overlap
            if(firstlog==1) firstlog=0;
            else p=p*y*2/cfacr*rc*rhol; //Accumulate probability for this
                //iteration according to the original circle radius
            psum+=p;//Accumulate probabilities for averaging over all iterations
            logpsum+=log(p);
            logpsumsq+=log(p)*log(p);
            if(firsttime==1) fprintf(ferr,"%lg %ld\n",p,k);//Diagnostics
            psumsq+=p*p; //For statistics of all iterations
            if(firsttime==1) //Diagnostic print for first case only
            {
                fprintf(ferr,"AMean= %lg GMean= %lg\n",psum/num,exp(logpsum/num));
                firsttime=0;
            }
            count++; //Increment case count
        }
        fprintf(fout,"%11.3lg%11.3lg\n",psum/num,exp(logpsum/num));
        //Output arithmetic and geometric mean for this case
    }
}

```

Input File "c:\temp\prden.in" 5/20/96

These inputs are the critical masses and critical radii, and are identical with the 10 cases listed in Ref. 5.43, Section 8. The critical masses are also given in Table 7.5-1 of this document.

cmass	rc
1.6	.574



10.1	1.4
2.5	0.685
10.1	1.4
6.5	0.98
7.4	1.17
18	1.7
55.2	2.18
11.1	1.2
30.9	1.65

The output file which shows the result of adjustment of the critical masses and radii (cmass and rc, respectively), and the resulting probability calculation, both arithmetic and geometric means, is given below.

Output file "c:\temp\prden.out", 5/20/1996

cmass	rc	Arith mean	Geom mean
0.520	0.394	0.000158	5.25e-014
3.283	0.961	3.71e-014	3.28e-029
0.813	0.470	9.63e-007	1.17e-017
3.283	0.961	8.31e-011	2.32e-029
2.112	0.673	1.52e-011	2.76e-029
2.405	0.803	1.43e-010	1.39e-026
5.850	1.167	1.52e-021	1.67e-040
17.940	1.496	1.03e-057	2.36e-089
3.608	0.824	4.7e-018	1.74e-038
10.042	1.133	7.18e-046	2.84e-071

The above results provide the probability of occurrence of a spherical reducing zone with sufficient organic material to remove a critical mass of uranium from a groundwater stream. The occurrence is for an arbitrary point in a horizontal layer which has the proper characteristics. The probability of actual occurrence of a critical mass involves the probability that a waste package containing sufficiently high fissile concentration will give rise to a groundwater plume which intersects the critical mass circle area, summed over all possible positions of this circle, and weighted by the fraction of the host rock which might be occupied by such a reducing zone (obtained from further analysis of the occurrence of orebodies on the Colorado Plateau) according to the methodology given in Section 7.6.

**Statistics for fossil logs found in the Club Group of Mines, Montrose County, CO**

The purpose of this attachment is to summarize the information obtained from Plate 57 of Reference 5.28 and to detail relevant statistics for use in the Attachment II and the body of the analysis. Reference 5.28, Plate 57 provides a detailed map of the geology of vanadium-bearing sandstones at the Club Group of Mines, in Montrose County Colorado. Figure III-1 presents a reduced copy of this map, with the areas of V-bearing sandstone divided into five sections. Each of the logs in each section have also been uniquely labeled with an alphabetical identifier. The length, distance to the nearest log (center-to-center), and distance to the next nearest log, have been measured for each log, and are summarized in Table III-1 below. All measurements were made using English units since the original map scale is in feet. However, conversion to SI is also provided in the table.

**Table III-1. Length and Separation Distance for Fossil Logs at the Club Mines, Montrose County, Colorado**

Section No.	Log No.	Distance to Nearest Neighbor		Distance to Next Nearest Neighbor		Log Length	
		feet	meters	feet	meters	feet	meters
1	A	231	70.41	231	70.41	47	14.33
1	B	113	34.44	213	64.92	69	21.03
1	C	113	34.44	200	60.96	31	9.45
1	D	200	60.96	213	64.92	38	11.58
1	E	25	7.62	125	38.1	31	9.45
1	F	25	7.62	144	43.89	25	7.62
2	A	6	1.83	69	21.03	16	4.88
2	B	6	1.83	63	19.2	19	5.79
2	C	63	19.2	69	21.03	75	22.86
2	D	16	4.88	63	19.2	22	6.71
2	E	16	4.88	75	22.86	19	5.79
2	F	69	21.03	313	95.4	19	5.79
2	G	69	21.03	256	78.03	16	4.88
3	A	9	2.74	31	9.45	13	3.96
3	B	9	2.74	31	9.45	19	5.79
3	C	31	9.45	31	9.45	16	4.88
3	D	88	26.82	131	39.93	25	7.62
3	E	50	15.24	75	22.86	28	8.53
3	F	35	10.67	38	11.58	38	11.58
3	G	25	7.62	35	10.67	19	5.79
3	H	25	7.62	38	11.58	16	4.88
3	I	69	21.03	106	32.31	25	7.62
3	J	38	11.58	69	21.03	50	15.24
3	K	38	11.58	106	32.31	31	9.45
3	L	78	23.77	97	29.57	22	6.71
3	M	97	29.57	125	38.1	25	7.62

Table III-1. Length and Separation Distance for Fossil Logs at the Club Mines, Montrose County, Colorado

Section No.	Log No.	Distance to Nearest Neighbor		Distance to Next Nearest Neighbor		Log Length	
		feet	meters	feet	meters	feet	meters
3	N	78	23.77	108	32.31	22	6.71
3	O	84	25.6	156	47.55	31	9.45
3	P	84	25.6	150	45.72	25	7.62
3	Q	100	30.48	150	45.72	19	5.79
3	R	100	30.48	200	60.96	19	5.79
3	S	275	83.82	363	110.64	22	6.71
3	T	200	60.96	238	72.54	13	3.96
3	U	6	1.83	50	15.24	6	1.83
3	V	6	1.83	44	13.41	13	3.96
3	W	44	13.41	50	15.24	19	5.79
3	X	41	12.5	44	13.41	16	4.88
3	Y	6	1.83	19	5.79	22	6.71
3	Z	13	3.96	19	5.79	16	4.88
3	AA	6	1.83	13	3.96	9	2.74
3	AB	13	3.96	16	4.88	13	3.96
3	AC	50	15.24	53	16.15	16	4.88
3	AD	69	21.03	69	21.03	28	8.53
3	AE	6	1.83	69	21.03	16	4.88
3	AF	6	1.83	71	21.64	16	4.88
3	AG	75	22.86	109	33.22	22	6.71
3	AH	38	11.58	75	22.86	19	5.79
3	AI	38	11.58	94	28.65	13	3.96
3	AJ	38	11.58	78	23.77	22	6.71
3	AK	9	2.74	53	16.15	16	4.88
3	AL	9	2.74	56	17.07	19	5.79
3	AM	53	16.15	56	17.07	13	3.96
3	AN	22	6.71	22	6.71	16	4.88
3	AO	9	2.74	9	2.74	16	4.88
3	AP	9	2.74	9	2.74	25	7.62
3	AQ	28	8.53	34	10.36	16	4.88
3	AR	50	15.24	56	17.07	13	3.96
3	AS	13	3.96	56	17.07	13	3.96
3	AT	13	3.96	69	21.03	19	5.79
3	AU	9	2.74	9	2.74	6	1.83
3	AV	38	11.58	109	33.22	19	5.79
3	AW	50	15.24	81	24.69	19	5.79
4	A	125	38.1	134	40.84	16	4.88
4	B	38	11.58	119	36.27	16	4.88
4	C	38	11.58	84	25.6	22	6.71
4	D	6	1.83	84	25.6	19	5.79
4	E	50	15.24	69	21.03	41	12.5
4	F	50	15.24	59	17.98	19	5.79
4	G	50	15.24	59	17.98	22	6.71
4	H	50	15.24	63	19.2	19	5.79

Table III-1. Length and Separation Distance for Fossil Logs at the Club Mines, Montrose County, Colorado

Section No.	Log No.	Distance to Nearest Neighbor		Distance to Next Nearest Neighbor		Log Length	
		feet	meters	feet	meters	feet	meters
4	I	63	19.2	88	26.82	9	2.74
4	J	31	9.45	88	26.82	28	8.53
4	K	31	9.45	63	19.2	16	4.88
4	L	56	17.07	81	24.69	60	18.29
4	M	56	17.07	97	29.57	25	7.62
4	N	31	9.45	69	21.03	72	21.95
4	O	31	9.45	38	11.58	25	7.62
4	P	31	9.45	38	11.58	19	5.79
4	Q	31	9.45	63	19.2	9	2.74
4	R	91	27.74	100	30.48	78	23.77
4	S	6	1.83	84	25.6	19	5.79
4	T	19	5.79	25	7.62	34	10.36
4	U	13	3.96	25	7.62	9	2.74
4	V	13	3.96	19	5.79	6	4.88
5	NO LOGS IN THIS SECTION						

In addition, the area of V-bearing sandstone in each section was estimated by determining the area of a polygon representative of the general shape of the curved V-bearing sandstone boundary (multiple polygons were used if the section contained more than one region of V-bearing sandstone), as shown in Figure III-2. The barren areas were excluded from the area estimates. These areas, along with the average log density (# logs in section/section area), log length, and separation distance, are given for each section, and for the total area of vanadium-bearing sandstone in Table III-2 below.

Table III-2. Vanadium Bearing Sandstone Section Areas and Averages

Section No.	No. of Logs	Estimated Section Area		Log Density		Average Distance to Nearest Log		Average Distance to Next Nearest Log		Average Log Length	
		ft <sup>2</sup>	m <sup>2</sup>	logs/ft <sup>2</sup>	logs/m <sup>2</sup>	ft	m	ft	m	ft	m
1	6	203937	18946	2.94E-05	3.17E-04	117.83	35.92	187.67	57.20	40.17	12.24
2	7	47363	4400	1.48E-04	1.59E-03	35.00	10.67	129.71	39.54	26.57	8.10
3	49	561389	52155	8.73E-05	9.40E-04	47.46	14.46	77.59	23.65	19.47	5.93
4	22	74911	6959	2.94E-04	3.16E-03	41.36	12.61	70.41	21.46	26.95	8.22
5	0	50170	4661	N/A	N/A	N/A	N/A	N/A	N/A	N/A	N/A
TOTAL	84	937770	87122	8.96E-05	9.64E-04	49.31	15.03	87.51	26.67	23.50	7.16

Figures III-3, III-4, and III-5 present distributions of the log lengths, distance to the nearest log, and distance to the next nearest log, respectively. The distribution of log length is of particular interest for critical mass estimates in Attachment II and

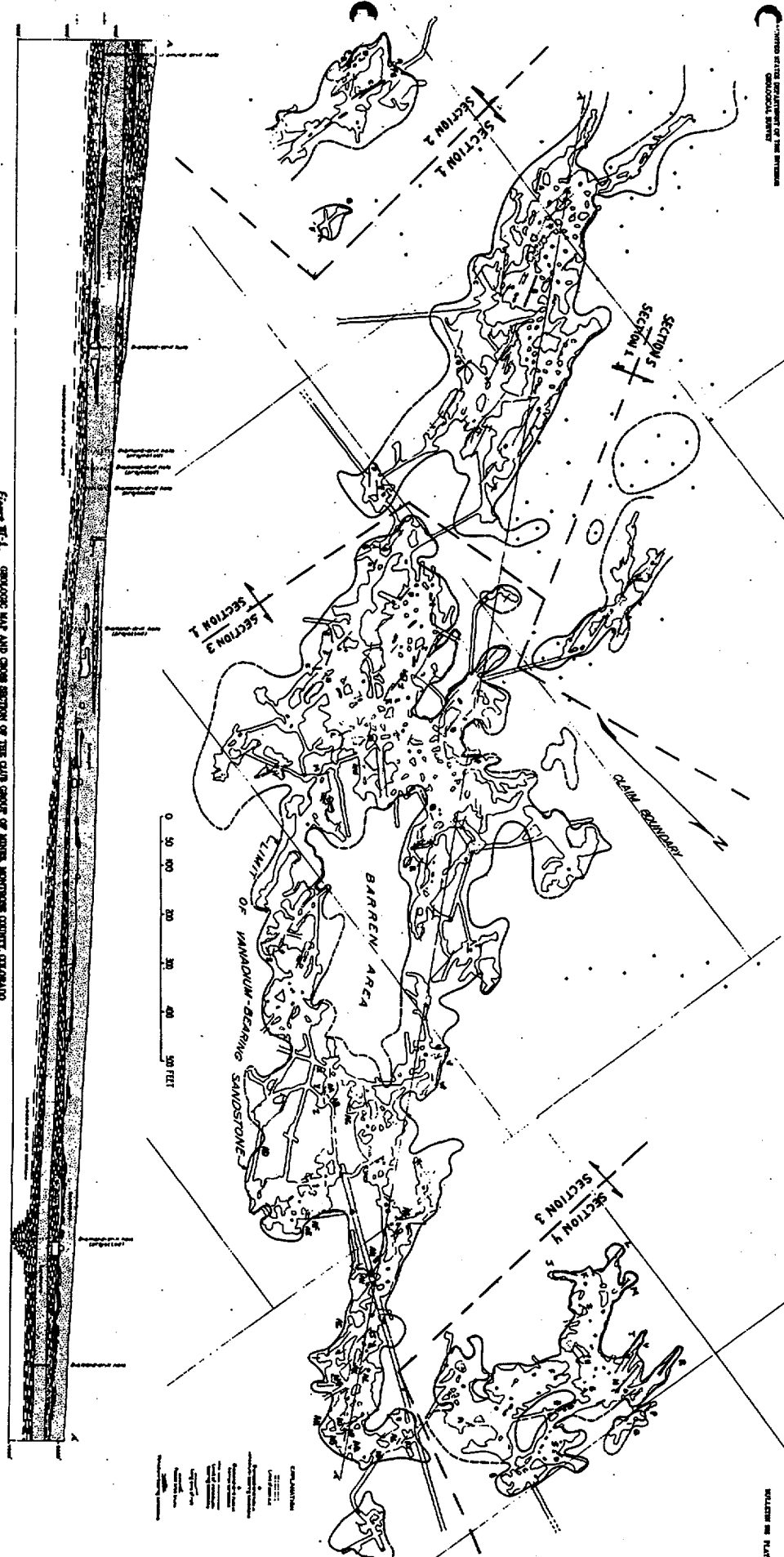


Figure III-1. GEOLOGIC MAP AND CROSS SECTION OF THE GLEN CANYON OF ARICA, MONTROSE COUNTY, COLORADO

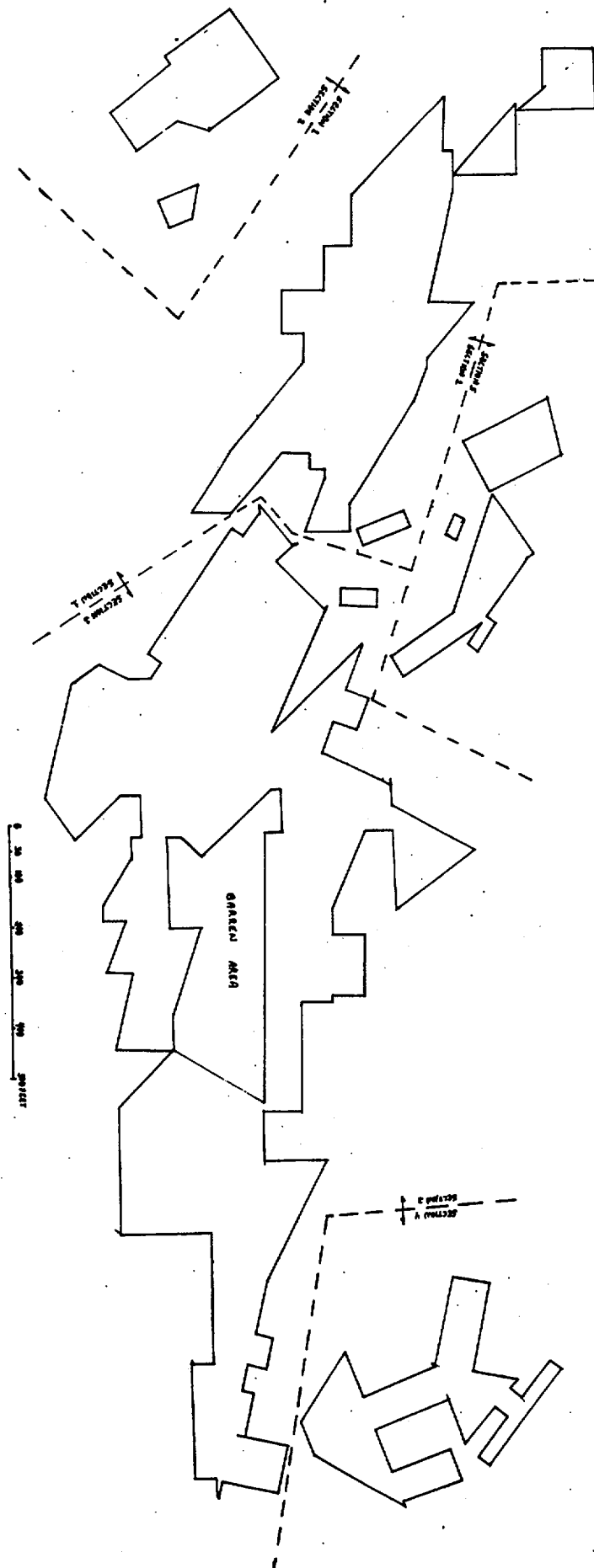


Figure III-2. Representative areas used for estimate of vanadium bearing sandstone areas in each section.

III-5

May 27, 1996  
21 50/10

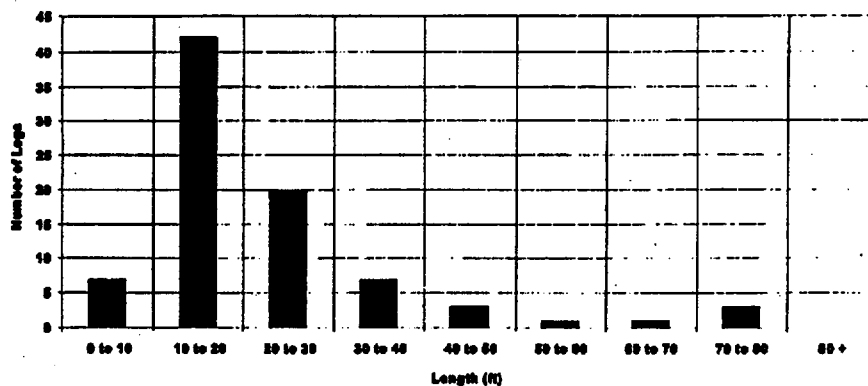


Figure III-3. Distribution of fossil log lengths at the Club Mines.

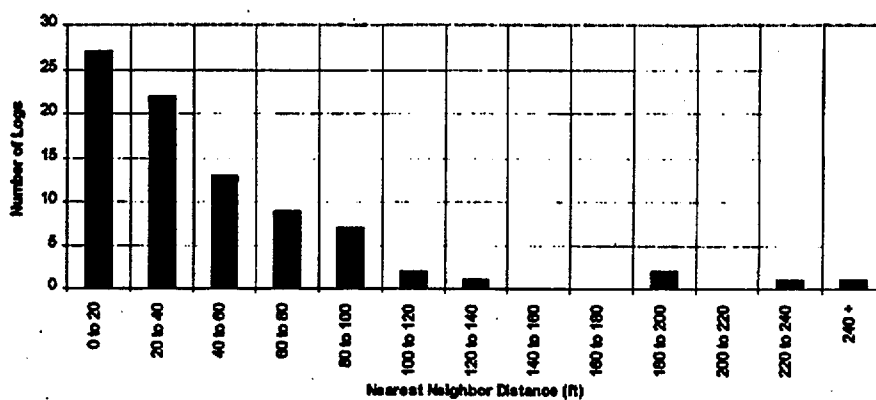


Figure III-4. distribution of distance from log center to center of nearest log.

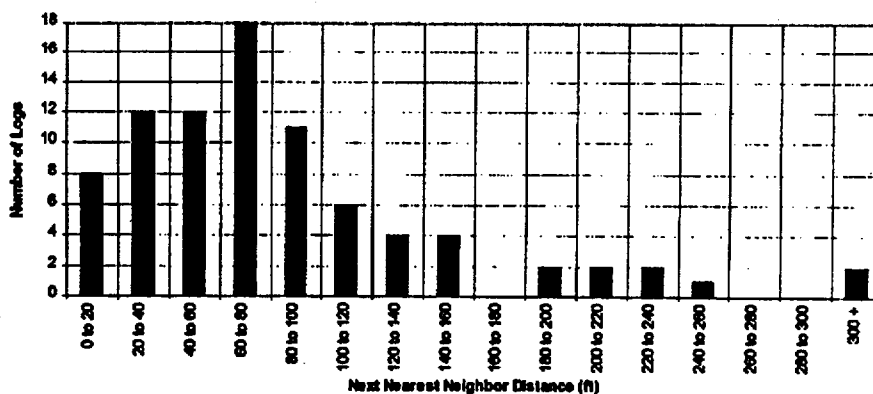


Figure III-5. Distribution of distance from log center to center of next nearest log.

the body of the report. Inspection of Figure III-3 indicates that for lengths greater than 10 feet, the log length distribution can be approximated by a negative exponential distribution. To test this hypothesis, the 84 log length samples were arranged in ascending order and those under 10 feet were eliminated (the first 7). The remaining 77 logs were each assigned a complementary cumulative probability using the parametric estimator

$$1-F(l_i) = [n-i+0.625]/[n+0.25],$$

where  $n$  is the sample size (77 logs), and  $i$  is the ranking of the individual log (1 smallest, 77 largest). As the floor of this distribution is taken to be 10 feet, this value must be subtracted from each log length ( $l = L-10$  ft). These steps are presented in Table III-3. For an exponential distribution,

$$\ln[1-F(l)] = -\lambda * l.$$

Therefore,  $\lambda$  can be determined by plotting the  $\ln[1-F(l)]$  vs.  $l$ , as is done in Figure III-6. Using the regression function of Microsoft Excel v5.0, this yields a  $\lambda$  of  $0.0656 \text{ ft}^{-1}$  ( $0.2152 \text{ m}^{-1}$ ) with an  $R^2$  of 0.93. This indicates that a negative exponential distribution provides an acceptable fit for fossil log lengths greater than 10 foot at the Club Group of Mines.

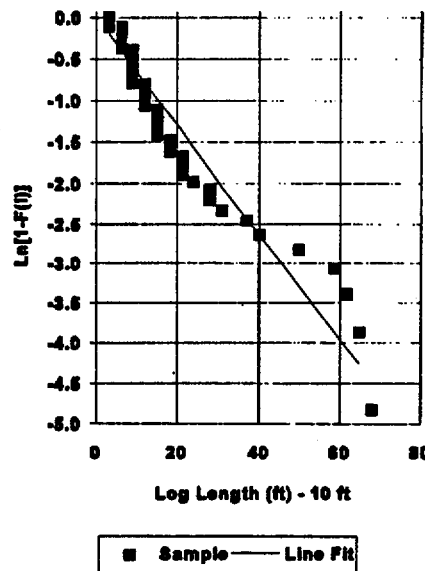


Figure III-6. Exponential fit of log length data.

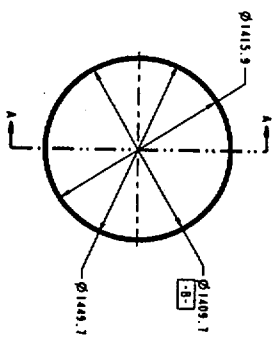


Table III-3. Exponential fit of log length data

i	L	i = L-10	1-F(i)	ln[1-F(i)]
1	13	3	0.9919	-0.0081
2	13	3	0.9790	-0.0213
3	13	3	0.9660	-0.0346
4	13	3	0.9531	-0.0481
5	13	3	0.9401	-0.0617
6	13	3	0.9272	-0.0756
7	13	3	0.9142	-0.0897
8	13	3	0.9013	-0.1039
9	16	6	0.8883	-0.1184
10	16	6	0.8754	-0.1331
11	16	6	0.8625	-0.1480
12	16	6	0.8495	-0.1631
13	16	6	0.8366	-0.1784
14	16	6	0.8236	-0.1940
15	16	6	0.8107	-0.2099
16	16	6	0.7977	-0.2260
17	16	6	0.7848	-0.2423
18	16	6	0.7718	-0.2590
19	16	6	0.7589	-0.2759
20	16	6	0.7460	-0.2931
21	16	6	0.7330	-0.3106
22	16	6	0.7201	-0.3284
23	16	6	0.7071	-0.3466
24	16	6	0.6942	-0.3650
25	19	9	0.6812	-0.3839
26	19	9	0.6683	-0.4030
27	19	9	0.6553	-0.4226
28	19	9	0.6424	-0.4426
29	19	9	0.6294	-0.4629
30	19	9	0.6165	-0.4837
31	19	9	0.6036	-0.5049
32	19	9	0.5906	-0.5266
33	19	9	0.5777	-0.5488
34	19	9	0.5647	-0.5714
35	19	9	0.5518	-0.5946
36	19	9	0.5388	-0.6183
37	19	9	0.5259	-0.6427
38	19	9	0.5129	-0.6676
39	19	9	0.5000	-0.6931

Table III-3. Exponential fit of log length data

I	L	I = L-10	1-F(I)	ln[1-F(I)]
40	19	9	0.4871	-0.7194
41	19	9	0.4741	-0.7463
42	19	9	0.4612	-0.7740
43	22	12	0.4482	-0.8025
44	22	12	0.4353	-0.8318
45	22	12	0.4223	-0.8620
46	22	12	0.4094	-0.8931
47	22	12	0.3964	-0.9252
48	22	12	0.3835	-0.9584
49	22	12	0.3706	-0.9928
50	22	12	0.3576	-1.0283
51	22	12	0.3447	-1.0652
52	25	15	0.3317	-1.1035
53	25	15	0.3188	-1.1433
54	25	15	0.3058	-1.1847
55	25	15	0.2929	-1.2280
56	25	15	0.2799	-1.2732
57	25	15	0.2670	-1.3205
58	25	15	0.2540	-1.3702
59	25	15	0.2411	-1.4225
60	28	18	0.2282	-1.4777
61	28	18	0.2152	-1.5361
62	28	18	0.2023	-1.5982
63	31	21	0.1893	-1.6643
64	31	21	0.1764	-1.7351
65	31	21	0.1634	-1.8114
66	31	21	0.1505	-1.8939
67	34	24	0.1375	-1.9838
68	38	28	0.1246	-2.0827
69	38	28	0.1117	-2.1924
70	41	31	0.0987	-2.3156
71	47	37	0.0858	-2.4562
72	50	40	0.0728	-2.6198
73	60	50	0.0599	-2.8156
74	69	59	0.0469	-3.0592
75	72	62	0.0340	-3.3820
76	75	65	0.0210	-3.8615
77	78	68	0.0081	-4.8171



**25 2 PLACES -**

SECTION A-A  
SCALE 0.060

**PRELIMINARY**  
-FOR INFORMATION ONLY-

Figure IV-1  
WAP AUCF Design  
(21-MKR) Inner Barrier

[illegible]

IV-1 May 31, 1996

Participant MO

Yucca Mtn. Site Char. Project-Planning & Control System  
PACS Participant Work Station (PPWS)  
Participant Planning Sheet (PSA03)

01-Sep-95 to

Prepared - 11/16/95:13:46:53

Inc. Dollars in Thousands

P&amp;S Account No. - 1.2.2.3.3 TR

P&amp;S Account Title - Uncanistered Spent Fuel

WBS No. - 1.2.2.3.3

WBS Title - Uncanistered Spent Fuel

BASELINE Start Date - 10/01/95  
BASELINE Finish Date - 09/30/96

Element ID - TR233

Annual Budget	Prior	Fiscal Year Distribution										Future	At Complete	
		FY1996	FY1997	FY1998	FY1999	FY2000	FY2001	FY2002	FY2003	FY2004	FY2005			
	0	1467	0	0	0	0	0	0	0	0	0	0	0	1467

## Statement of Work:

The following quality affecting work shall be controlled in accordance with approved implementing procedures identified on the current OCRWM-accepted Requirements Traceability Network Matrix.

QARD applies to this effort.

## OBJECTIVE:

Design waste packages to accommodate spent nuclear fuel that may arrive at the repository in an uncanistered form or fuel that must be repackaged. Produce drawings and specifications for Advanced Conceptual Design (ACD) and Investment Analysis (IAD). Conduct analyses to support waste package design development.

## DESCRIPTION:

All efforts required to:

- Perform analyses of waste package components, including alternative concepts or features required to support the design process. Technical and economic analyses will be performed using models and computer codes. Technical analyses will include structural, shielding, criticality, thermal, and component performance analyses to determine the adequacy of various design concepts.
- Develop the waste package design drawings and specifications documents for both ACD and IAD. Participate in design reviews necessary for each design phase.
- Develop interface drawings and specifications in support of the subsurface and surface design efforts.

## FY 1996 Scope of Work:

Continue to develop waste package designs to accommodate uncanistered spent nuclear fuel and non-fuel bearing waste stream forms. Evaluate the waste package uncanistered spent fuels using industry standards and processes including high and low thermal loads, spent nuclear fuel temperatures, shielding (source development), structural, and criticality. Investigate different waste streams generated at utilities (fuel and non-fuel bearing spent nuclear fuel). Develop design mitigation solutions (i.e., filler material and supplemental neutron absorber materials). Prepare initial Investment Analysis drawings/sketches for the uncanistered spent fuel waste package. Update, verify and validate, and maintain analytical computers and computer codes.

Initiate the calculation of keff for a family of spent nuclear fuel age, and for burn-up and enrichments for boiling water reactor and pressurized water reactor fuel. Establish keff for the family of waste package designs.

Prepared - 11/16/95:13:46:53

P&amp;S Account No. - 1.2.2.3.3 TR

-Uncanistered Spent Fuel

## Statement of Work (cont.):

Prepare and support design review documentation and presentation materials describing waste package design features to support review of the Mined Geologic Disposal System Advanced Conceptual Design. Design three cut-away waste package models, an uncanistered waste package model, a small multi-purpose canister disposal container with multi-purpose canister, and a high-level waste package model as appropriate.

Apply probabilistic methods to evaluate compliance of engineered Barrier Segment designs with regulatory requirements. Provide guidance for waste package design based on evaluations of direct hazards to the waste package. Provide guidance for the design of backfill, invert, and other non-waste package components of the Engineered Barrier Segment. Identify/define design basis accidents and events that affect the waste package or engineered barrier system, in coordination with Systems Engineering, Performance Assessment and Repository Design.

Perfect and use: (1) failure modes and effects analysis for each waste package and Engineered Barrier Segment design to identify credible failure modes for each component, the mechanisms and conditions necessary to produce the identified failure modes, and the effects of the failure on other components of the waste package; (2) comprehensive configuration generator for the evaluation of the probability associated with all credible event sequences that can lead to configurations likely to cause waste package system failures. All probabilities associated with environmental parameters will be obtained from models developed by, or in association with, CRMS M&O Performance Assessment.

The configurations identified will be evaluated deterministically with respect to the appropriate waste package system failures. For criticality, additional probabilistic evaluations will be applied to the determination of consequences reflecting the uncertainty of environmental parameters that affect the duration of the criticality.

Develop and use probabilistic models of fuel dissolution, fuel transport by ground water, and re-precipitation. All activities will be coordinated with CRMS M&O Performance Assessment and will use the Waste Forms Characteristics Report as a reference.

Support the development of acceptance criteria for DOE spent nuclear fuel. Identify potential problems with respect to the appropriate acceptance criteria. Perform analyses to determine waste package parameter modifications necessary to meet these criteria. All activities will be performed in coordination with appropriate staff at Idaho National Engineering Laboratory and under the auspices of the repository task team of the DOE Spent Fuel Steering Committee.

Investigate disposal criticality issues and evaluate the draft technical report issued in September 1995 relating to the Engineered Barrier Segment. Prepare and submit the second draft of the Disposal Criticality Technical Report. Support technical exchanges with the Nuclear Regulatory Commission to solicit comments regarding criticality issues.

Monitor the ongoing testing programs, including the 29 principal isotopes required for disposal criticality, and participate in the decision process directing the isotopic testing program. Seek out reactor restart reactor core neutronic data to benchmark the neutronics computers codes.

## DELIVERABLES

Deliv ID	Description/Completion criteria	Due Date

Participant MO

Yucca Mtn. Site Char. Project-Planning & Control System  
PACS Participant Work Station (PPWS)  
Participant Planning Sheet (PSA03)

01-Sep-95 to 30-Sep-95

Page

Inc. Dollars in Thousands

Prepared - 11/16/95:13:46:53

P&amp;S Account No. - 1.2.2.3.3 TR -Unanistered Spent Fuel

## DELIVERABLES

Deliv ID	Description/Completion criteria	Due Date
ALT6224		
ALT6225	<p>Probabalistic Extrnl Criticality Eval (First Drft)</p> <p>Criteria - Documents the probabilistic evaluation of criticalities external to the waste package arising from fissile material released from the engineered barrier system. This report will also include summaries of related environmental parameter information provided by Performance Assessment.</p> <p>The due date will be met, and 90% of earned value applied, upon submittal to the M&amp;O Plans and Procedures Department. The remaining 10% of earned value will be applied upon review and acceptance by YHSCO. If no review comments are received from DOE within 30 days of receipt of the document by DOE, the remaining 10% earned value may be applied.</p>	31-May-96

Participant NO

Yucca Mtn. Site Char. Project-Planning & Control System  
PACS Participant Work Station (PPWS)  
Participant Planning Sheet (PSA03)

01-Sep-95

Prepared - 11/16/95:13:46:53

Inc. Dollars in T

P&S Account No. - 1.2.2.3.3 TR

-Uncanistered Spent Fuel

Approvals

RD Spell 11/16/95  
Preparer - print name Date  
[Signature]  
Preparer - Signature

R. L. Crann  
Technical Reviewer - print name  
R. L. Crann 11/17/95  
Technical Reviewer - Signature Date

Richard A. Kettell 11/24/95  
QA Reviewer - print name Date  
Richard A. Kettell 11/24/95  
QA Reviewer - Signature Date